

Radiative corrections to the $\tau^- \rightarrow (P_1 P_2)^- \nu_\tau$ ($P_{1,2} = \pi, K$) decays

Rafel Escribano^{1,2,*}, Jesús Alejandro Miranda^{2,†} and Pablo Roig^{3,‡}

¹*Grup de Física Teòrica, Departament de Física,
Universitat Autònoma de Barcelona, 08193 Bellaterra (Barcelona), Spain.*

²*Institut de Física d'Altes Energies (IFAE) and
The Barcelona Institute of Science and Technology,
Campus UAB, 08193 Bellaterra (Barcelona), Spain.*

³*Departamento de Física, Centro de Investigación y de
Estudios Avanzados del Instituto Politécnico Nacional,
Apdo. Postal 14-740, 07000 Ciudad de México, México.*

Abstract

The radiative corrections to the $\tau^- \rightarrow (P_1 P_2)^- \nu_\tau$ ($P_{1,2} = \pi, K$) decays are calculated for the first time including the structure-dependent real photon corrections, which are obtained using Resonance Chiral Theory. Our results, whose uncertainty is dominated by the model-dependence of the resummation of the radiative corrections and the missing virtual structure-dependent contributions, allow for precise tests of CKM unitarity, lepton flavour universality and non-standard interactions.

Keywords: Effective Field Theories, Semileptonic decays, Tau decays

* rescriba@ifae.es

† jmiranda@ifae.es

‡ proig@fis.cinvestav.mx

INTRODUCTION

Semileptonic tau decays are well-known to be a clean laboratory for studying QCD hadronic matrix elements at energies below ~ 1.8 GeV [1, 2], where the light-flavoured resonances play a key role. All non-perturbative information of the one-meson tau decays is encoded in the corresponding P decay constants, that are best determined in lattice QCD [3]. Two-meson tau decays are specified in terms of two form factors, whose knowledge has improved over the years thanks to the use of dispersion relations [4–16] and nourished with high quality measurements [17–24]. A similar good understanding has not yet been achieved in three-meson tau decays [8, 25–33] or higher-multiplicity modes, preventing for the moment their use in searches for new physics.

On the contrary, one- and two-meson tau decays have enabled significant and promising new physics tests in recent years [34–46]. At the precision attained, radiative corrections for these decay modes become necessary, which motivated their improved evaluation for the $\tau^- \rightarrow P^- \nu_\tau$ cases [43, 44, 47–49]. For the di-pion tau decays, the need for these corrections first stemmed from their use in the dispersive integral rendering the leading order hadronic vacuum polarization contribution to the muon $g - 2$ [50–52], which was again the target of our recent analysis [53] (see also Refs. [54–56]). Ref. [11] put forward that, assuming lepton universality, semileptonic kaon decay measurements could be used to predict the corresponding (crossing-symmetric) tau decays, yielding a V_{us} determination closer to unitarity than with the tau decay branching ratios. In that work, the model-independent radiative corrections were taken into account and the structure-dependent ones were estimated (see also Ref. [57]), resulting in a relative large (conservative) uncertainty. Including these model-dependent effects is one of our main motivations: here we focus on those with a real photon and defer the virtual photon ones to a later dedicated study. Instead of relying on lepton universality and checking CKM unitarity [11], one can in principle test the latter, comparing the crossed channels, or directly bind new physics non-standard interactions from $\tau^- \rightarrow (K\pi)^- \nu_\tau$ decays [38]. For completeness, we also include the radiative corrections to the di-kaon tau decays and recall our reference results for the di-pion mode [53]. As noted in Ref. [46], see Fig. 1 for instance, bounds on non-standard interactions from hadronic tau decays are competitive and complementary to those coming from LHC searches and electroweak precision observables. As a relevant example, the precise comparison of $\tau \rightarrow \pi^- \pi^0 \nu_\tau(\gamma)$ with $e^+ e^- \rightarrow \pi^+ \pi^-(\gamma)$ data, which requires the radiative corrections computed in this work (see also Ref. [53]), are able to reduce the allowed new physics area (in the relevant Wilson coefficients plane) by a factor ~ 3 [46].

Real radiation was computed for the $\tau^- \rightarrow \eta^{(\prime)}\pi^- \nu_\tau$ decay channels in Ref. [58], showing that it can contend with the non-photon decays, as G -parity and electromagnetic suppressions compete. Finally, we also estimate the corresponding results for the $K^- \eta^{(\prime)}$ channels.

The structure of the paper is as follows. In section I, we recall the model-independent description of the $\tau^- \rightarrow P_1^- P_2^0 \nu_\tau \gamma$ decays and give the leading real-photon model-dependent corrections for the $K\pi$, $K\bar{K}$ and $\pi\pi$ cases, where only the latter are known (see e.g. Refs. [51, 53]). Branching ratios and spectra for the radiative decays are analysed in section III, and the corresponding radiative correction factors are computed in section IV. We show the consequences of including them in section V, where we bind new physics couplings in an effective approach. Finally, we conclude in section VI. Appendices cover $K_{\ell 3}$ decays (A), structure-independent virtual corrections to di-meson tau decays (B), the non-radiative decays (C), and the kinematics of these three- and four-body processes (D).

I. THE $\tau^- \rightarrow P_1^- P_2^0 \nu_\tau \gamma$ DECAYS

The most general structure for the decays $\tau(P) \rightarrow P_1^-(p_-) P_2^0(p_0) \nu_\tau(q') \gamma(k)$ is given by

$$\begin{aligned} \mathcal{M} = & \frac{eG_F V_{uD}^*}{\sqrt{2}} \epsilon_\mu^* \left[\frac{H_V(p_-, p_0)}{k^2 - 2k \cdot P} \bar{u}(q') \gamma^\nu (1 - \gamma^5) (m_\tau + \not{P} - \not{k}) \gamma^\mu u(P) \right. \\ & \left. + (V^{\mu\nu} - A^{\mu\nu}) \bar{u}(q') \gamma_\nu (1 - \gamma^5) u(P) \right], \end{aligned} \quad (1)$$

with V_{uD} ($D = d, s$) the corresponding CKM matrix element and where the hadronic matrix element can be written as

$$H^\nu(p_-, p_0) = C_V F_+(t) Q^\nu + C_S \frac{\Delta_{-0}}{t} q^\nu F_0(t), \quad (2)$$

with $t = q^2$, $Q^\nu = (p_- - p_0)^\nu - \frac{\Delta_{-0}}{t} q^\nu$, $q^\nu = (p_- + p_0)^\nu$, and $\Delta_{ij} = m_i^2 - m_j^2$. One recovers the usual definition of $H_{K\pi}^\nu$ [38] by replacing $p_- \rightarrow p_K$, $p_0 \rightarrow p_\pi$ and $\Delta_{-0} \rightarrow \Delta_{K\pi}$ for $K^- \pi^0$, and $p_- \rightarrow p_\pi$, $p_0 \rightarrow p_K$, $C_{V,S} \rightarrow -C_{V,S}$ and $\Delta_{-0} \rightarrow -\Delta_{K\pi}$ for $\bar{K}^0 \pi^-$ (we comment on the identifications for the $P_1 = P_2$ channels below). In all cases, gauge invariance implies $k_\mu V^{\mu\nu} = H^\nu(p_-, p_0)$ and $k_\mu A^{\mu\nu} = 0$.

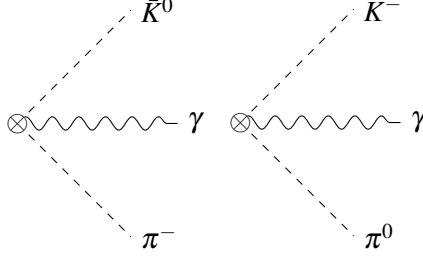


FIG. 1. Feynman diagrams contributing to the term proportional to the metric tensor $g^{\mu\nu}$ in Eq. (3).

The structure-independent term is given by

$$\begin{aligned}
V_{\text{SI}}^{\mu\nu} &= \frac{H^\nu(p_- + k, p_0)(2p_- + k)^\mu}{2k \cdot p_- + k^2} - C_V \frac{F_+(t') - F_+(t)}{k \cdot q} Q^\nu q^\mu \\
&+ \left\{ -C_V F_+(t') - \frac{\Delta_{-0}}{t'} [C_S F_0(t') - C_V F_+(t')] \right\} g^{\mu\nu} \\
&+ \frac{\Delta_{-0}}{tt'} \left\{ 2 [C_S F_0(t') - C_V F_+(t')] - \frac{C_S t'}{k \cdot q} [F_0(t') - F_0(t)] \right\} q^\mu q^\nu,
\end{aligned} \tag{3}$$

where $C_V^{K^- \pi^0} = C_S^{K^- \pi^0} = 1/\sqrt{2}$ for the $K^- \pi^0$ channel, and $C_V^{\bar{K}^0 \pi^-} = C_S^{\bar{K}^0 \pi^-} = -1$ for the $\bar{K}^0 \pi^-$ one, with $t' = (P - q')^2$. The main difference between these two decay modes comes from the overall sign difference—except for the first term in the second line of Eq. (3)—, that we absorbed in our definition of $C_{V,S}^{\bar{K}^0 \pi^-}$, and through the order of the arguments of H^ν in the above equation. At leading order (LO) in Chiral Perturbation Theory (ChPT), contributions proportional to $g^{\mu\nu}$ in $V_{\text{SI}}^{\mu\nu}$ stem from the diagrams in Fig. 1.

For the other tau decay modes, $V_{\text{SI}}^{\mu\nu}$ is also obtained from Eq. (3). In particular, we are also interested in the $\tau^- \rightarrow K^- K^0 \nu_\tau \gamma$ decays, where $C_V^{K^- K^0} = C_S^{K^- K^0} = -1$ ¹.

The structure-dependent part is given by

$$\begin{aligned}
V_{\text{SD}}^{\mu\nu} &= v_1(k \cdot p_- g^{\mu\nu} - k^\nu p_-^\mu) + v_2(k \cdot p_0 g^{\mu\nu} - k^\nu p_0^\mu) \\
&+ v_3(k \cdot p_0 p_-^\mu - k \cdot p_- p_0^\mu) p_-^\nu + v_4(k \cdot p_0 p_-^\mu - k \cdot p_- p_0^\mu) (p_- + p_0 + k)^\nu,
\end{aligned} \tag{4}$$

and

$$\begin{aligned}
A_{\mu\nu} &= ia_1 \varepsilon_{\mu\nu\rho\sigma} (p_0 - p_-)^\rho k^\sigma + ia_2 (P - q')_\nu \varepsilon_{\mu\rho\sigma\tau} k^\rho p_-^\sigma p_0^\tau \\
&+ ia_3 \varepsilon_{\mu\nu\rho\sigma} k^\rho (P - q')^\sigma + ia_4 (p_0 + k)_\nu \varepsilon_{\mu\lambda\rho\sigma} k^\lambda p_-^\rho p_0^\sigma,
\end{aligned} \tag{5}$$

¹ We discuss briefly the $\pi^- \pi^0$ case at the end of Sec. II 1; see Ref. [53] for further details.

where p_- and p_0 refer to the momentum of the charged and neutral meson, respectively.

From Eq. (3), it is easy to show that the Low's theorem [59] is manifestly satisfied,

$$\begin{aligned}
V^{\mu\nu} &= \frac{p_-^\mu}{k \cdot p_-} H^\nu(p_-, p_0) + \left\{ C_V F_+(t) + \frac{\Delta_{-0}}{t} [C_S F_0(t) - C_V F_+(t)] \right\} \left(\frac{p_-^\mu k^\nu}{k \cdot p_-} - g^{\mu\nu} \right) \\
&\quad - \frac{2\Delta_{-0}}{t^2} [C_S F_0(t) - C_V F_+(t)] \left(\frac{k \cdot p_0}{k \cdot p_-} p_-^\mu - p_0^\mu \right) (p_- + p_0)^\nu \\
&\quad + 2 \left(\frac{k \cdot p_0}{k \cdot p_-} p_-^\mu - p_0^\mu \right) \left[C_V \frac{dF_+(t)}{dt} Q^\nu + C_S \frac{\Delta_{-0}}{t} q^\nu \frac{dF_0(t)}{dt} \right] + \mathcal{O}(k),
\end{aligned} \tag{6}$$

and the amplitude reads

$$\begin{aligned}
\mathcal{M} &= \frac{e G_F V_{ud} \sqrt{S_{EW}}}{\sqrt{2}} \varepsilon_\mu^*(k) H_\nu(p_-, p_0) \bar{u}(q) \gamma^\nu (1 - \gamma^5) u(P) \\
&\quad \times \left(\frac{p_-^\mu}{k \cdot p_- + \frac{1}{2} M_\gamma^2} - \frac{P^\mu}{k \cdot P - \frac{1}{2} M_\gamma^2} \right) + \mathcal{O}(k^0),
\end{aligned} \tag{7}$$

where S_{EW} encodes the short-distance electroweak corrections [60–67].

In the Low's limit, one gets

$$\begin{aligned}
|\overline{\mathcal{M}}|^2 &= 2e^2 G_F^2 |V_{ud}|^2 S_{EW} \left\{ C_S^2 |F_0(t)|^2 D_0^{P^- P^0}(t, u) + C_S C_V \text{Re} [F_+(t) F_0^*(t)] D_{+0}^{P^- P^0}(t, u) \right. \\
&\quad \left. + C_V^2 |F_+(t)|^2 D_+^{P^- P^0}(t, u) \right\} \sum_{\gamma \text{ pols.}} \left| \frac{p_- \cdot \varepsilon}{p_- \cdot k} - \frac{P \cdot \varepsilon}{P \cdot k} \right|^2 + \mathcal{O}(k^0),
\end{aligned} \tag{8}$$

where

$$\begin{aligned}
D_+^{P^- P^0}(t, u) &= \frac{m_\tau^2}{2} (m_\tau^2 - t) + 2m_0^2 m_-^2 - 2u(m_\tau^2 - t + m_0^2 + m_-^2) + 2u^2 \\
&\quad + \frac{\Delta_{-0}}{t} m_\tau^2 (2u + t - m_\tau^2 - 2m_0^2) + \frac{\Delta_{-0}^2}{t^2} \frac{m_\tau^2}{2} (m_\tau^2 - t),
\end{aligned} \tag{9}$$

$$D_0^{P^- P^0}(t, u) = \frac{\Delta_{-0}^2 m_\tau^4}{2t^2} \left(1 - \frac{t}{m_\tau^2} \right), \tag{10}$$

$$D_{+0}^{P^- P^0}(t, u) = \frac{\Delta_{-0} m_\tau^2}{t} \left[2u + t - m_\tau^2 - 2m_0^2 + \frac{\Delta_{-0}}{t} (m_\tau^2 - t) \right], \tag{11}$$

with $u = (P - p_-)^2$. In this way, besides the Low theorem, the Burnett-Kroll theorem [68] is also explicitly manifest.

Thus, after integration over neutrino and photon 4-momenta, the differential decay width in this approximation reads

$$\begin{aligned} \left. \frac{d\Gamma^{(0)}}{dt du} \right|_{PP\gamma} &= \frac{G_F^2 |V_{uD}|^2 S_{EW}}{128\pi^3 m_\tau^3} \left\{ C_S^2 |F_0(t)|^2 D_0^{P^-P^0}(t, u) + C_V C_S \text{Re} [F_+^*(t) F_0(t)] D_{+0}^{P^-P^0}(t, u) \right. \\ &\quad \left. + C_V^2 |F_+(t)|^2 D_+^{P^-P^0}(t, u) \right\} g_{\text{rad}}(t, u, M_\gamma), \end{aligned} \quad (12)$$

where (see Refs. [50, 51])

$$g_{\text{rad}}(t, u, M_\gamma) = g_{\text{brems}}(t, u, M_\gamma) + g_{\text{rest}}(t, u), \quad (13)$$

with

$$g_{\text{brems}}(t, u, M_\gamma) = \frac{\alpha}{\pi} (J_{11}(t, u, M_\gamma) + J_{20}(t, u, M_\gamma) + J_{02}(t, u, M_\gamma)), \quad (14a)$$

$$g_{\text{rest}}(t, u) = \frac{\alpha}{\pi} (K_{11}(t, u) + K_{20}(t, u) + K_{02}(t, u)). \quad (14b)$$

The relevant expressions for $J_{ij}(t, u, M_\gamma)$ and $K_{ij}(t, u)$, which correspond to an integration over \mathcal{D}^{III} and $\mathcal{D}^{\text{IV/III}}$, respectively, can be found in Refs. [11, 51, 53] and in App. D².

Integrating upon the u variable in Eq. (12), one gets

$$\begin{aligned} \left. \frac{d\Gamma}{dt} \right|_{\text{III}} &= \frac{G_F^2 S_{EW} |V_{uD}|^2 m_\tau^3}{384\pi^3 t} \left\{ \frac{1}{2t^2} \left(1 - \frac{t}{m_\tau^2}\right)^2 \lambda^{1/2}(t, m_-^2, m_0^2) \right. \\ &\quad \left. \times \left[C_V^2 |F_+(t)|^2 \left(1 + \frac{2t}{m_\tau^2}\right) \lambda(t, m_-^2, m_0^2) \bar{\delta}_+(t) + 3C_S^2 \Delta_{-0}^2 |F_0(t)|^2 \bar{\delta}_0(t) \right] + C_S C_V \frac{4}{\sqrt{t}} \bar{\delta}_{+0}(t) \right\}, \end{aligned} \quad (15)$$

with

$$\bar{\delta}_0(t) = \frac{\int_{u^-(t)}^{u^+(t)} D_0^{P^-P^0}(t, u) g_{\text{brems}}(t, u, M_\gamma) du}{\int_{u^-(t)}^{u^+(t)} D_0^{P^-P^0}(t, u) du}, \quad (16a)$$

$$\bar{\delta}_+(t) = \frac{\int_{u^-(t)}^{u^+(t)} D_+^{P^-P^0}(t, u) g_{\text{brems}}(t, u, M_\gamma) du}{\int_{u^-(t)}^{u^+(t)} D_+^{P^-P^0}(t, u) du}, \quad (16b)$$

$$\bar{\delta}_{+0}(t) = \frac{3t\sqrt{t}}{4m_\tau^6} \int_{u^-(t)}^{u^+(t)} D_{+0}^{P^-P^0}(t, u) g_{\text{brems}}(t, u, M_\gamma) \text{Re} [F_+^*(t) F_0(t)] du. \quad (16c)$$

The remaining contribution, $d\Gamma/dt|_{\text{IV/III}}$, which corresponds to the integration over $\mathcal{D}^{\text{IV/III}}$ with $g_{\text{rest}}(t, u)$ instead of $g_{\text{brems}}(t, u, M_\gamma)$, is almost negligible and only becomes relevant near threshold. In Ref. [69], the subleading contributions in the Low's approximation were studied, showing that they are not negligible and need to be taken into account to get a reliable estimation.

² The function $K_{11}(t, u)$ turns out to be numerically negligible and is not quoted anywhere; see e.g. Refs [36, 50].

II. STRUCTURE-DEPENDENT CONTRIBUTIONS

The evaluation of the structure-dependent tensors, $V_{SD}^{\mu\nu}$ and $A^{\mu\nu}$ in eqs. (4) and (5), requires non-perturbative methods or lattice QCD (which has only been explored for the $\pi\pi$ case, see [70]). The tau lepton mass value probes the hadronization of QCD currents in its semileptonic decays beyond the regime of validity of Chiral Perturbation Theory [71–75] (χPT), which is the low-energy effective field theory of QCD describing P meson physics. To extend the applicability of the chiral Lagrangians to the energy region where meson states resonate, a successful strategy has been to include the corresponding fields as explicit degrees of freedom into the action, using approximate flavor symmetry, without additional assumptions affecting the possible resonance dynamics [76, 77]. This procedure was later christened Resonance Chiral Theory ($R\chi T$, see e.g. ref. [78]) and yields as a result the saturation of the χPT low-energy constants upon resonance integration.

Explicitly, the construction of the relevant Lagrangian pieces including resonances uses the chiral tensors [75] (we only quote those relevant in our computation)

$$\begin{aligned} u_\mu &= i [u^\dagger (\partial_\mu - ir_\mu)u - u(\partial_\mu - i\ell_\mu)u^\dagger], \\ f_\pm^{\mu\nu} &= uF_L^{\mu\nu}u^\dagger \pm u^\dagger F_R^{\mu\nu}u, \\ \chi_\pm &= u^\dagger \chi u^\dagger \pm u\chi u, \end{aligned} \tag{17}$$

where the pseudo-Goldstone bosons are included in u via (λ_a are the Gell-Mann matrices, so that $\phi^3 = \pi^0$ in the isospin symmetry limit)

$$u = \exp\left(\frac{i\Phi}{\sqrt{2}f}\right), \quad \Phi = \sum_{a=0}^8 \frac{\lambda_a}{\sqrt{2}}\phi^a, \tag{18}$$

and left- and right-handed sources ℓ_μ and r_μ enter through

$$F_X^{\mu\nu} = \partial^\mu x^\nu - \partial^\nu x^\mu - i[x^\mu, x^\nu] = eQF^{\mu\nu} + \dots, \quad x = \ell, r; \quad Q = \text{diag}\left(\frac{2}{3}, -\frac{1}{3}, -\frac{1}{3}\right), \tag{19}$$

with $x_\mu = eQA_\mu + \dots$, being A_μ the photon field and $F^{\mu\nu} = \partial^\mu A^\nu - \partial^\nu A^\mu$ the corresponding field-strength tensor. Spin-zero sources (s and p) appear in χ_\pm through $\chi = 2B(s + ip)$, where we recall that the two leading chiral low-energy constants (f and B) determine the light-quark condensate in the chiral limit, $-Bf^2 = \langle 0|\bar{q}q|0 \rangle$, with $f \sim 90$ MeV the pion decay constant. The numerical value of B is not needed, as it only enters the pseudoscalar meson squared masses, which are

proportional to it. Indeed, in the isospin symmetry limit, $\text{diag}(2Bs) = (m_\pi^2, m_\pi^2, 2m_K^2 - m_\pi^2)$, where s accounts for the (diagonal) light-quark mass matrix, which ensure chiral symmetry breaking as in QCD.

The $R\chi T$ Lagrangian includes the lowest order χPT Lagrangian in both parity sectors, which is

$$\mathcal{L}_{\text{non-res}}^{\text{even}} = \frac{f^2}{4} \langle u^\mu u_\mu + \chi_+ \rangle, \quad \mathcal{L}_{\text{non-res}}^{\text{odd}} = \mathcal{L}_{\text{WZW}}, \quad (20)$$

where WZW stands for the chiral anomaly contribution worked out by Wess-Zumino and Witten [79, 80].

In addition, $\mathcal{L}_{R\chi T}$ has pieces including resonance fields and chiral tensors. These are usually incorporated taking into account the order (within the chiral counting) of their contributions -upon resonance exchange- to the χPT couplings [76, 77, 81, 82], as well as their behaviour [83] in the limit of a large number of colors [84, 85]. QCD asymptotic behaviour forbids (linear combinations of) operators with increasing number of derivatives. In this way $R\chi T$ bridges between the low-energy behaviour of χPT and the high-energy constraints of perturbative QCD, keeping predictivity for a set of related observables, to a given precision, without unnecessary assumptions (like, for instance vector meson dominance [86] or any additional symmetry of gauge type related to them [87]). Within this framework, the need for non-resonant contributions was explored e. g. in ref. [88] for the $\omega - \pi^0$ transition form factor, where it was found that they could play a rôle above 2 GeV only. Taking this into account and the fact that we are limited kinematically by the tau mass, we neglect non-resonant pieces in the following.

Apart from contributions that are suppressed by approximate flavor symmetries (more on this below), the next-to-leading order χPT couplings are saturated by spin-one resonance exchange [76, 77] coming from the following operators

$$\mathcal{L}_V = \frac{F_V}{2\sqrt{2}} \langle V_{\mu\nu} f_+^{\mu\nu} \rangle + i \frac{G_V}{2\sqrt{2}} \langle V_{\mu\nu} [u^\mu, u^\nu] \rangle, \quad \mathcal{L}_A = \frac{F_A}{2\sqrt{2}} \langle A_{\mu\nu} f_-^{\mu\nu} \rangle, \quad (21)$$

where $V_{\mu\nu} = \sum_{a=0}^8 \frac{\lambda^a}{\sqrt{2}} V_{\mu\nu}^a$, and analogously for the axial-vector resonances. For convenience, spin-one resonances are worked out in the antisymmetric tensor field formalism [76, 77]. For completeness we note that the kinetic terms come from the Lagrangian (which also includes interactions, hidden in the covariant derivative, that are however not needed in what follows, so $\nabla^\alpha \sim \partial^\alpha$)

$$\mathcal{L}_{\text{Res}}^{\text{Kin}} = -\frac{1}{2} \langle \nabla_\lambda V^{\lambda\nu} \nabla^\rho V_{\rho\nu} \rangle + \frac{M_V^2}{4} \langle V_{\mu\nu} V^{\mu\nu} \rangle, \quad (22)$$

with obvious replacements for axial-vector resonances, $A_{\mu\nu}$.

$U(3)$ symmetry in the (axial-)vector resonance masses is broken by operators of the form $\langle V_{\mu\nu}V^{\mu\nu}\chi_+ \rangle$, $V \leftrightarrow A$ [89–91], which can accommodate the measured spectra (in this way we will simply replace the different spin-one resonance masses by the PDG values [92] in the following). Analogously, breaking of this flavor symmetry also affects $F_{V,A}$. However, in the vector case, the coupling giving this shift ³[81] is constrained by short-distance QCD to vanish within the scheme considered in ref. [93] (see also ref. [88], where these contributions were neglected *a priori*). Based on this, flavor symmetry on $F_{V,A}$ is assumed in the remainder of the paper.

All resonance contributions to the v_i form factors (those to the a_i are differed by one chiral order and thus neglected) depend on ratios of resonance couplings over the meson decay constant $\left(\frac{F_V G_V}{f^2}, \frac{F_V^2}{f^2}, \frac{F_A^2}{f^2}\right)$, which are constrained by asymptotic QCD. Therefore the well-known $SU(3)$ symmetry breaking which causes $f_K \sim 1.2f_\pi$ [92] cannot be accounted for, within the considered simplified scheme, without conflicting with short-distance QCD requirements. Thus, we are using $f \sim 90$ MeV for the v_i also in the strangeness-changing channels ⁴. The dispersive constructions giving the $F_{+,0}$ form factors account for flavor symmetry breaking in the $K\pi$ channels, as required by the precision of the corresponding measurements, which fed the phaseshifts entering the dispersive integrals.

1. Vector contributions

Including those Lagrangian terms that, upon resonance integration, contribute to the ChPT $\mathcal{O}(p^4)$ low-energy constants (LECs), we have found the following contributions to the vector form factors v_i in Eq. (4), which are depicted in Fig. 2:

$$\begin{aligned} v_1 = & \frac{F_V G_V}{\sqrt{2}f^2 M_\rho^2} \left\{ \left(1 + \frac{1}{3} \frac{M_\rho^2}{M_\omega^2} + \frac{2}{3} \frac{M_\rho^2}{M_\phi^2} \right) \left[1 + \frac{1}{2} (t - \Delta_{K\pi}) D_{K^*}^{-1}(t) \right] \right. \\ & \left. + 2M_\rho^2 D_{K^*}^{-1}(t') + M_\rho^2 (t - \Delta_{K\pi}) D_{K^*}^{-1}(t) D_{K^*}^{-1}(t') \right\} \\ & + \frac{F_V^2}{2\sqrt{2}f^2 M_\rho^2} \left[-\frac{1}{2} \left(1 + \frac{1}{3} \frac{M_\rho^2}{M_\omega^2} + \frac{2}{3} \frac{M_\rho^2}{M_\phi^2} \right) (1 - t' D_{K^*}^{-1}(t')) - M_\rho^2 D_{K^*}^{-1}(t') \right] \end{aligned}$$

³ It is λ_6^V in the notation of ref. [81] and λ_V in ref. [93], with $\lambda_6^V = \frac{\lambda_V}{\sqrt{2}}$.

⁴ The associated error is, however, much smaller than the uncertainty that we will find in our results, see section IV.

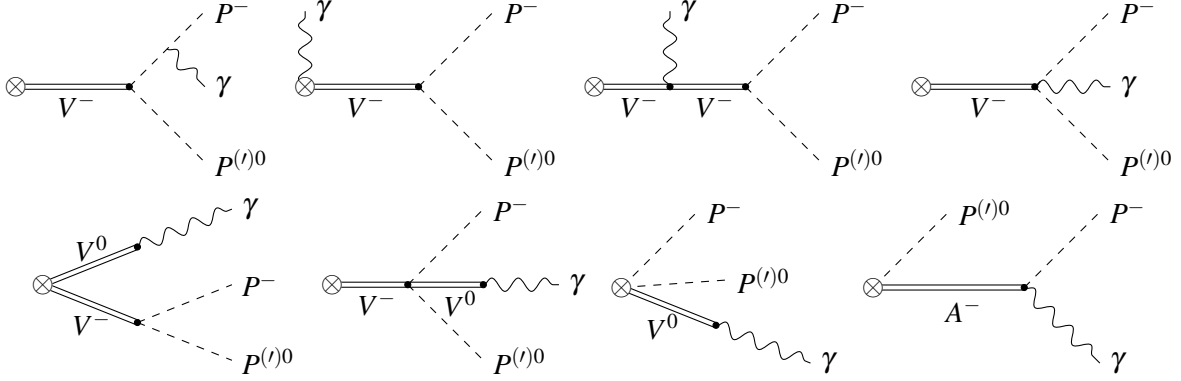


FIG. 2. Vector and axial-vector meson exchange diagrams contributing to the $\tau^- \rightarrow P_1^- P_2^0 \nu_\tau \gamma$ decays at $\mathcal{O}(p^4)$. V^0 stands for the ρ^0 , ω and ϕ resonances, $V^- = K^{*-}$ for the $K\pi$ modes and $V^- = \rho^-$ for the $K^- K^0$ one, and $A^- = K_1^-$ in $K^- K^0$ and $K^- \pi^0$, and $A^- = a_1^-$ in $\pi^- \bar{K}^0$.

$$+ \frac{F_A^2}{\sqrt{2} f^2 M_{K_1}^2} \left(M_{K_1}^2 - \frac{1}{2} \Sigma_{K\pi} + \frac{1}{2} t \right) D_{K_1}^{-1}[(p_K + k)^2], \quad (23a)$$

$$v_2 = \frac{F_V G_V}{\sqrt{2} f^2 M_\rho^2} (t + \Delta_{K\pi}) \left[-\frac{1}{2} \left(1 + \frac{1}{3} \frac{M_\rho^2}{M_\omega^2} + \frac{2}{3} \frac{M_\rho^2}{M_\phi^2} \right) D_{K^*}^{-1}(t) - M_\rho^2 D_{K^*}^{-1}(t) D_{K^*}^{-1}(t') \right]$$

$$+ \frac{F_V^2}{2\sqrt{2} f^2 M_\rho^2} \left[-\frac{1}{2} \left(1 + \frac{1}{3} \frac{M_\rho^2}{M_\omega^2} + \frac{2}{3} \frac{M_\rho^2}{M_\phi^2} \right) (1 + t' D_{K^*}^{-1}(t')) - M_\rho^2 D_{K^*}^{-1}(t') \right]$$

$$+ \frac{F_A^2}{\sqrt{2} f^2 M_{K_1}^2} (M_{K_1}^2 - m_K^2 - k \cdot p_K) D_{K_1}^{-1}[(p_K + k)^2], \quad (23b)$$

$$v_3 = \frac{F_A^2}{\sqrt{2} f^2 M_{K_1}^2} D_{K_1}^{-1}[(p_K + k)^2], \quad (23c)$$

$$v_4 = -\frac{2F_V G_V}{\sqrt{2} f^2} D_{K^*}^{-1}(t) D_{K^*}^{-1}(t') + \frac{F_V^2}{2\sqrt{2} f^2 M_\rho^2} \left(1 + \frac{1}{3} \frac{M_\rho^2}{M_\omega^2} + \frac{2}{3} \frac{M_\rho^2}{M_\phi^2} \right) D_{K^*}^{-1}(t'), \quad (23d)$$

for $K^- \pi^0$,

$$v_1 = -\frac{F_V G_V}{f^2 M_\rho^2} \left[2 + 2M_\rho^2 D_{K^*}^{-1}(t') + \frac{1}{2} \left(1 + \frac{1}{3} \frac{M_\rho^2}{M_\omega^2} + \frac{2}{3} \frac{M_\rho^2}{M_\phi^2} \right) (t + \Delta_{K\pi}) D_{K^*}^{-1}(t) \right.$$

$$\left. + (t + \Delta_{K\pi}) M_\rho^2 D_{K^*}^{-1}(t) D_{K^*}^{-1}(t') \right]$$

$$- \frac{F_V^2}{2f^2 M_\rho^2} \left[-M_\rho^2 D_{K^*}^{-1}(t') + \frac{1}{2} \left(1 + \frac{1}{3} \frac{M_\rho^2}{M_\omega^2} + \frac{2}{3} \frac{M_\rho^2}{M_\phi^2} \right) t' D_{K^*}^{-1}(t') + \frac{1}{2} \left(-3 + \frac{1}{3} \frac{M_\rho^2}{M_\omega^2} + \frac{2}{3} \frac{M_\rho^2}{M_\phi^2} \right) \right]$$

$$-\frac{F_A^2}{f^2 M_{a_1}^2} \left(M_{a_1}^2 - \frac{1}{2} \Sigma_{K\pi} + \frac{1}{2} t \right) D_{a_1}^{-1} [(p\pi + k)^2], \quad (24a)$$

$$\begin{aligned} v_2 = & -\frac{F_V G_V}{f^2 M_\rho^2} \left\{ (t - \Delta_{K\pi}) \left[-M_\rho^2 D_{K^*}^{-1}(t) D_{K^*}^{-1}(t') - \frac{1}{2} \left(1 + \frac{1}{3} \frac{M_\rho^2}{M_\omega^2} + \frac{2}{3} \frac{M_\rho^2}{M_\phi^2} \right) D_{K^*}^{-1}(t) \right] \right. \\ & \left. + 1 - \frac{1}{3} \frac{M_\rho^2}{M_\omega^2} - \frac{2}{3} \frac{M_\rho^2}{M_\phi^2} \right\} \\ & -\frac{F_V^2}{2f^2 M_\rho^2} \left[-M_\rho^2 D_{K^*}^{-1}(t') - \frac{1}{2} \left(1 + \frac{1}{3} \frac{M_\rho^2}{M_\omega^2} + \frac{2}{3} \frac{M_\rho^2}{M_\phi^2} \right) t' D_{K^*}^{-1}(t') + \frac{1}{2} \left(-3 + \frac{1}{3} \frac{M_\rho^2}{M_\omega^2} + \frac{2}{3} \frac{M_\rho^2}{M_\phi^2} \right) \right] \\ & -\frac{F_A^2}{f^2 M_{a_1}^2} (M_{a_1}^2 - m_\pi^2 k \cdot p_\pi) D_{a_1}^{-1} [(p\pi + k)^2], \end{aligned} \quad (24b)$$

$$v_3 = -\frac{F_A^2}{f^2 M_{a_1}^2} D_{a_1}^{-1} [(p\pi + k)^2], \quad (24c)$$

$$v_4 = \frac{2F_V G_V}{f^2} D_{K^*}^{-1}(t) D_{K^*}^{-1}(t') - \frac{F_V^2}{2f^2 M_\rho^2} \left(1 + \frac{1}{3} \frac{M_\rho^2}{M_\omega^2} + \frac{2}{3} \frac{M_\rho^2}{M_\phi^2} \right) D_{K^*}^{-1}(t'), \quad (24d)$$

for $\bar{K}^0 \pi^-$, and

$$\begin{aligned} v_1 = & -\frac{F_V G_V}{f^2 M_\rho^2} \left[1 + \frac{1}{3} \frac{M_\rho^2}{M_\omega^2} + \frac{2}{3} \frac{M_\rho^2}{M_\phi^2} + (t - \Delta_{K^- K^0}) D_\rho^{-1}(t) + 2M_\rho^2 D_\rho^{-1}(t') \right. \\ & \left. + M_\rho^2 (t - \Delta_{K^- K^0}) D_\rho^{-1}(t) D_\rho^{-1}(t') \right] \\ & -\frac{F_V^2}{2f^2 M_\rho^2} \left[-\frac{1}{3} \frac{M_\rho^2}{M_\omega^2} - \frac{2}{3} \frac{M_\rho^2}{M_\phi^2} + t' D_\rho^{-1}(t') - M_\rho^2 D_\rho^{-1}(t') \right] \\ & -\frac{F_A^2}{f^2 M_{K_1}^2} \left(M_{K_1}^2 - \frac{1}{2} \Sigma_{K^- K^0} + \frac{1}{2} t \right) D_{K_1}^{-1} [(p_- + k)^2], \end{aligned} \quad (25a)$$

$$\begin{aligned} v_2 = & -\frac{F_V G_V}{f^2 M_\rho^2} \left[-1 + \frac{1}{3} \frac{M_\rho^2}{M_\omega^2} + \frac{2}{3} \frac{M_\rho^2}{M_\phi^2} - (t + \Delta_{K^- K^0}) D_\rho^{-1}(t) - M_\rho^2 (t + \Delta_{K^- K^0}) D_\rho^{-1}(t) D_\rho^{-1}(t') \right] \\ & -\frac{F_V^2}{2f^2 M_\rho^2} \left[-\frac{1}{3} \frac{M_\rho^2}{M_\omega^2} - \frac{2}{3} \frac{M_\rho^2}{M_\phi^2} - t' D_\rho^{-1}(t') - M_\rho^2 D_\rho^{-1}(t') \right] \\ & -\frac{F_A^2}{f^2 M_{K_1}^2} (M_{K_1}^2 - m_{K^-}^2 - k \cdot p_-) D_{K_1}^{-1} [(p_- + k)^2], \end{aligned} \quad (25b)$$

$$v_3 = -\frac{F_A^2}{f^2 M_{K_1}^2} D_{K_1}^{-1} [(p_- + k)^2], \quad (25c)$$

$$v_4 = \frac{2F_V G_V}{f^2} D_\rho^{-1}(t) D_\rho^{-1}(t') - \frac{F_V^2}{f^2 M_\rho^2} D_\rho^{-1}(t'), \quad (25d)$$

for $K^- K^0$, where $\Sigma_{-0} = m_-^2 + m_0^2$ and $D_R(x) = M_R^2 - x - iM\Gamma_R(x)$. Off-shell resonance widths⁵ are given in terms of the leading pseudo-Goldstone boson cuts [26, 27, 94].

It is straightforward to show that, except for a Clebsch-Gordan coefficient (CGC) factor, one recovers the expressions found in Refs. [51, 53] for the vector form factors of the $\tau^- \rightarrow \pi^- \pi^0 \nu_\tau \gamma$ decays in the isospin-symmetry limit.

All the former resonance contributions are given in terms of three couplings: F_V , responsible for instance of the coupling of the vector resonance to the vector current; F_A for the couplings of the axial resonance; and G_V which yields, among others, vertices between the vector resonance and a couple of pseudo-Goldstone bosons (see e.g. Ref. [76] for further details).

2. Axial contributions

The Feynman diagrams that contribute to these decays are depicted in Figs. 3–5. At $\mathcal{O}(p^4)$, the axial form factors a_i in Eq. (5), which receive contributions from the Wess-Zumino-Witten functional [79, 80], are given by

$$a_1 = \frac{N_c}{12\sqrt{2}\pi^2 f^2}, \quad a_2 = -\frac{N_c}{6\sqrt{2}\pi^2 f^2 (t' - m_K^2)}, \quad a_3 = -\frac{N_c}{24\sqrt{2}\pi^2 f^2}, \quad (26)$$

for $K^- \pi^0$,

$$a_3 = -\frac{N_c}{24\pi^2 f^2}, \quad (27)$$

for $\bar{K}^0 \pi^-$, and

$$a_3 = \frac{N_c}{24\pi^2 f^2}, \quad (28)$$

for $K^- K^0$, where $N_c = 3$ is the number of colours and f is the pion decay constant in the chiral limit, $f \sim 90$ MeV.

In Fig. 5, only one diagram contributes to the $\tau^- \rightarrow K^- K^0 \nu_\tau \gamma$ decays similarly to the $\tau^- \rightarrow \bar{K}^0 \pi^- \nu_\tau \gamma$ decays. This is because the $K^- \rightarrow \bar{K}^0 \pi^- \gamma$ (or $\pi^- \rightarrow K^- K^0 \gamma$) vertex is absent in the WZW Lagrangian⁶. We reproduce the known anomalous contributions [51, 53] for the $\tau^- \rightarrow \pi^- \pi^0 \nu_\tau \gamma$ case. We neglect resonance contributions in the anomalous sector, which start at $\mathcal{O}(p^6)$ in the chiral power counting [82].

⁵ The on-shell width corresponds to the imaginary part of the pole position of the resonance. The imaginary part of the corresponding loop function provides an off-shell width function, which extends off the pole [94].

⁶ This feature was already studied for the $K_{\ell 3}$ decays in Ref. [95], where the non-local kaon pole term is only present in $A_{\mu\nu}^+$ for $K^+ \rightarrow \pi^0 \ell^+ \nu_\ell \gamma$ decays.

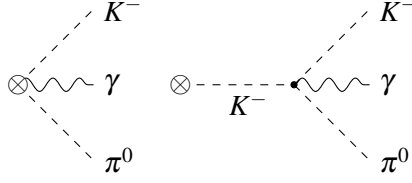


FIG. 3. Axial contributions to the $\tau^- \rightarrow K^- \pi^0 \nu_\tau \gamma$ decays at $\mathcal{O}(p^4)$.

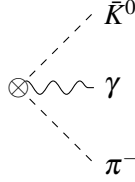


FIG. 4. Axial contributions to the $\tau^- \rightarrow \bar{K}^0 \pi^- \nu_\tau \gamma$ decays at $\mathcal{O}(p^4)$.

III. RADIATIVE HADRONIC TAU DECAYS

The differential rate for the $\tau^- \rightarrow P_1^- P_2^0 \nu_\tau \gamma$ decays in the τ rest frame is given by

$$d\Gamma = \frac{(2\pi)^4}{4m_\tau} \sum_{\text{spin}} \overline{|\mathcal{M}|^2} d\Phi_4, \quad (29)$$

where $d\Phi_4$ is the corresponding 4-body phase space, given by

$$d\Phi_4 = \delta^{(4)}(P - p_- - p_0 - q' - k) \frac{d^3 p_-}{(2\pi)^3 2E_-} \frac{d^3 p_0}{(2\pi)^3 2E_0} \frac{d^3 q'}{(2\pi)^3 2E_\nu} \frac{d^3 k}{(2\pi)^3 2E_\gamma}, \quad (30)$$

and $\overline{|\mathcal{M}|^2}$ is the unpolarized spin-averaged squared amplitude. Inasmuch as this amplitude is not IR finite, we follow the same procedure as in Refs. [51, 53] where a photon energy cut, E_γ^{cut} , was introduced to study the dynamics of the $\tau^- \rightarrow \pi^- \pi^0 \nu_\tau \gamma$ decays.

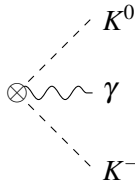


FIG. 5. Axial contributions to the $\tau^- \rightarrow K^- K^0 \nu_\tau \gamma$ decays at $\mathcal{O}(p^4)$.

E_γ^{cut}	Br(Low)	BR(SI)	BR($F_V = \sqrt{2}F$) [$\mathcal{O}(p^4)$]	BR($F_V = \sqrt{3}F$) [$\mathcal{O}(p^4)$]
100 MeV	3.4×10^{-6}	3.0×10^{-6}	3.5×10^{-6}	3.8×10^{-6}
300 MeV	6.2×10^{-7}	3.4×10^{-7}	6.3×10^{-7}	9.4×10^{-7}
500 MeV	7.4×10^{-8}	3.5×10^{-8}	1.5×10^{-7}	3.3×10^{-7}

TABLE I. Branching ratios $\text{Br}(\tau^- \rightarrow K^- \pi^0 \nu_\tau \gamma)$ for different values of E_γ^{cut} . The third column corresponds to the complete bremsstrahlung, and the fourth and fifth to the $\mathcal{O}(p^4)$ contributions.

E_γ^{cut}	Br(Low)	BR(SI)	BR($F_V = \sqrt{2}F$) [$\mathcal{O}(p^4)$]	BR($F_V = \sqrt{3}F$) [$\mathcal{O}(p^4)$]
100 MeV	2.6×10^{-5}	1.4×10^{-5}	1.6×10^{-5}	1.6×10^{-5}
300 MeV	6.2×10^{-6}	1.1×10^{-6}	1.7×10^{-6}	1.9×10^{-6}
500 MeV	1.0×10^{-6}	7.1×10^{-8}	2.0×10^{-7}	2.4×10^{-7}

TABLE II. Branching ratios $\text{Br}(\tau^- \rightarrow \bar{K}^0 \pi^- \nu_\tau \gamma)$ for different values of E_γ^{cut} . The third column corresponds to the complete bremsstrahlung, and the fourth and fifth to the $\mathcal{O}(p^4)$ contributions.

In this analysis, we call ‘‘complete bremsstrahlung’’ or simply ‘‘SI’’ the amplitude with $v_{1,2,3,4} = a_{1,2,3,4} = 0$. For the $\mathcal{O}(p^4)$ contributions, as in Ref. [53], we distinguish between using the set of short-distance constraints $F_V = \sqrt{2}F$, $G_V = F/\sqrt{2}$ [77] and $F_A = F$; or $F_V = \sqrt{3}F$, $G_V = F/\sqrt{3}$ and $F_A = \sqrt{2}F$ [81, 82, 96, 97]. The former corresponds to the constraints from 2-point Green functions and the second to the values consistent up to 3-point Green functions, which include operators that contribute at $\mathcal{O}(p^6)$ (that we are not including in this work). The difference between both sets of constraints has been employed to estimate roughly the model-dependent error of this approach [43, 44, 49, 53, 91]. In all our subsequent analyses, the $\mathcal{O}(p^4)$ results include the SI part and the structure dependent part (either with the $F_V = \sqrt{2}F$ or with the $F_V = \sqrt{3}F$ set of constraints).

Integrating Eq. (29) using the dispersive vector and scalar form factors [6, 7, 9, 13, 14, 98–100], we get the $P_1^- P_2^0$ invariant mass distribution, the photon energy distribution and the branching fraction as a function of E_γ^{cut} . The outcomes are depicted in Figs. 6, 7, 8 and 9, and summarized in Tables I, II and III.

The branching fractions of the radiative decays as a function of E_γ^{cut} are shown in Fig. 6. In Tables I and II, one can see that for $E_\gamma^{\text{cut}} \lesssim 100 \text{ MeV}$ the main contribution at $\mathcal{O}(p^4)$ comes from

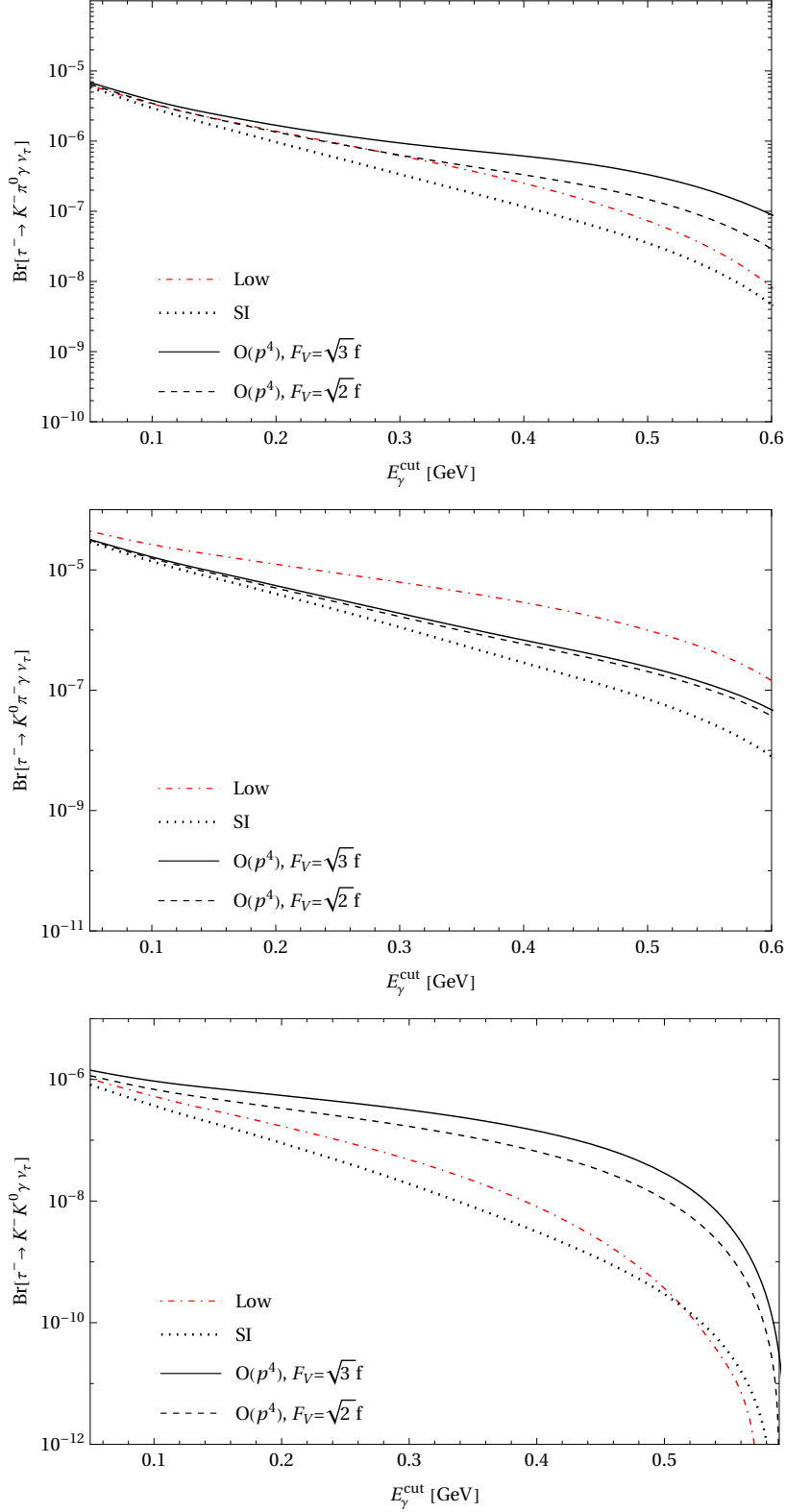


FIG. 6. Branching ratio for the $\tau^- \rightarrow K^- \pi^0 \nu_\tau \gamma$ (top), the $\tau^- \rightarrow \bar{K}^0 \pi^- \nu_\tau \gamma$ (centre) and the $\tau^- \rightarrow K^- K^0 \nu_\tau \gamma$ (bottom) decays as a function of E_γ^{cut} . The dotted line represents the bremsstrahlung contribution, the solid line and dashed line represent the $\mathcal{O}(p^4)$ corrections using $F_V = \sqrt{3}F$ and $F_V = \sqrt{2}F$, respectively. The red one corresponds to the Low approximation. 15

E_γ^{cut}	BR(Low)	BR(SI)	BR($F_V = \sqrt{2}F$) [$\mathcal{O}(p^4)$]	BR($F_V = \sqrt{3}F$) [$\mathcal{O}(p^4)$]
100 MeV	5.3×10^{-7}	3.7×10^{-7}	6.8×10^{-7}	9.4×10^{-7}
300 MeV	4.8×10^{-8}	1.9×10^{-8}	1.7×10^{-7}	3.1×10^{-7}
500 MeV	3.7×10^{-10}	3.0×10^{-10}	1.1×10^{-8}	2.9×10^{-8}

TABLE III. Branching ratios $\text{Br}(\tau^- \rightarrow K^- K^0 \nu_\tau \gamma)$ for different values of E_γ^{cut} . The third column corresponds to the complete bremsstrahlung, and the fourth and fifth to the $\mathcal{O}(p^4)$ contributions.

the complete bremsstrahlung (SI) amplitude in agreement with the results in Refs. [51, 53, 55] for the $\tau^- \rightarrow \pi^- \pi^0 \nu_\tau \gamma$ decays (see also the recent ref. [101]). It is also seen that the Low's approximation is sufficient to describe the $K^- \pi^0$ decays up to these energies, while this is not the case for the $\bar{K}^0 \pi^-$ ones. Contrary to the $\tau^- \rightarrow (K\pi)^- \nu_\tau$ transitions, where the $K^- \pi^0$ and $\pi^- \bar{K}^0$ decay modes differ only by a squared CGC factor in the isospin symmetry limit, the radiative decays are more subtle. At low photon energies, these two modes are approximately related by $\text{Br}(\tau^- \rightarrow \bar{K}^0 \pi^- \nu_\tau \gamma) / \text{Br}(\tau^- \rightarrow K^- \pi^0 \nu_\tau \gamma) \approx 2(m_K/m_\pi) \sim 7$, which explains their hierarchy. In both decay channels, the SD contributions seem to be subdominant, while the $\tau^- \rightarrow K^- K^0 \nu_\tau \gamma$ decays are more susceptible to these contributions (see Table III).

In Fig. 7, the decay spectrum is depicted with $v_i = a_i = 0$ for different E_γ^{cut} values. For the $\tau^- \rightarrow (K\pi)^- \nu_\tau \gamma$ decays, the first peak is due to bremsstrahlung off the charged meson, i.e. K^- or π^- , and the second one receives contributions from bremsstrahlung off the τ lepton and resonance exchange. In Fig. 8, we compare the distributions for $E_\gamma^{\text{cut}} = 300 \text{ MeV}$ using the Low's approximation (red dashed line), the SI amplitude (dotted line), and the $\mathcal{O}(p^4)$ amplitude with $F_V = \sqrt{2}F$ (dashed line) and $F_V = \sqrt{3}F$ (solid line). The most important contribution for the $(K\pi)^-$ decay channels comes from the $K^*(892)$ resonance exchange around $s \sim 0.79 \text{ GeV}^2$. It is worth noting that for the $\tau^- \rightarrow \bar{K}^0 \pi^- \nu_\tau \gamma$ decays, there is a huge suppression around the $K^*(892)$ peak when the full distribution is compared to the Low one. The reason for that is the following. While the Low approximation in Eq. (7) includes only the $\mathcal{O}(k^{-1})$ dominant contributions from the bremsstrahlung off the initial tau lepton and the final charged meson, the full amplitude in Eq. (1) contains also the $\mathcal{O}(k^0)$ subdominant contribution from the first line of this equation, which is common to both $(K\pi)^-$ channels, plus all the $\mathcal{O}(k^0)$ contributions from Eq. (6). Among the latter, the leading numerical contribution comes from the first term in the second line of Eq. (3), which has different sign depending on the channel, as already mentioned after that equation. This fact

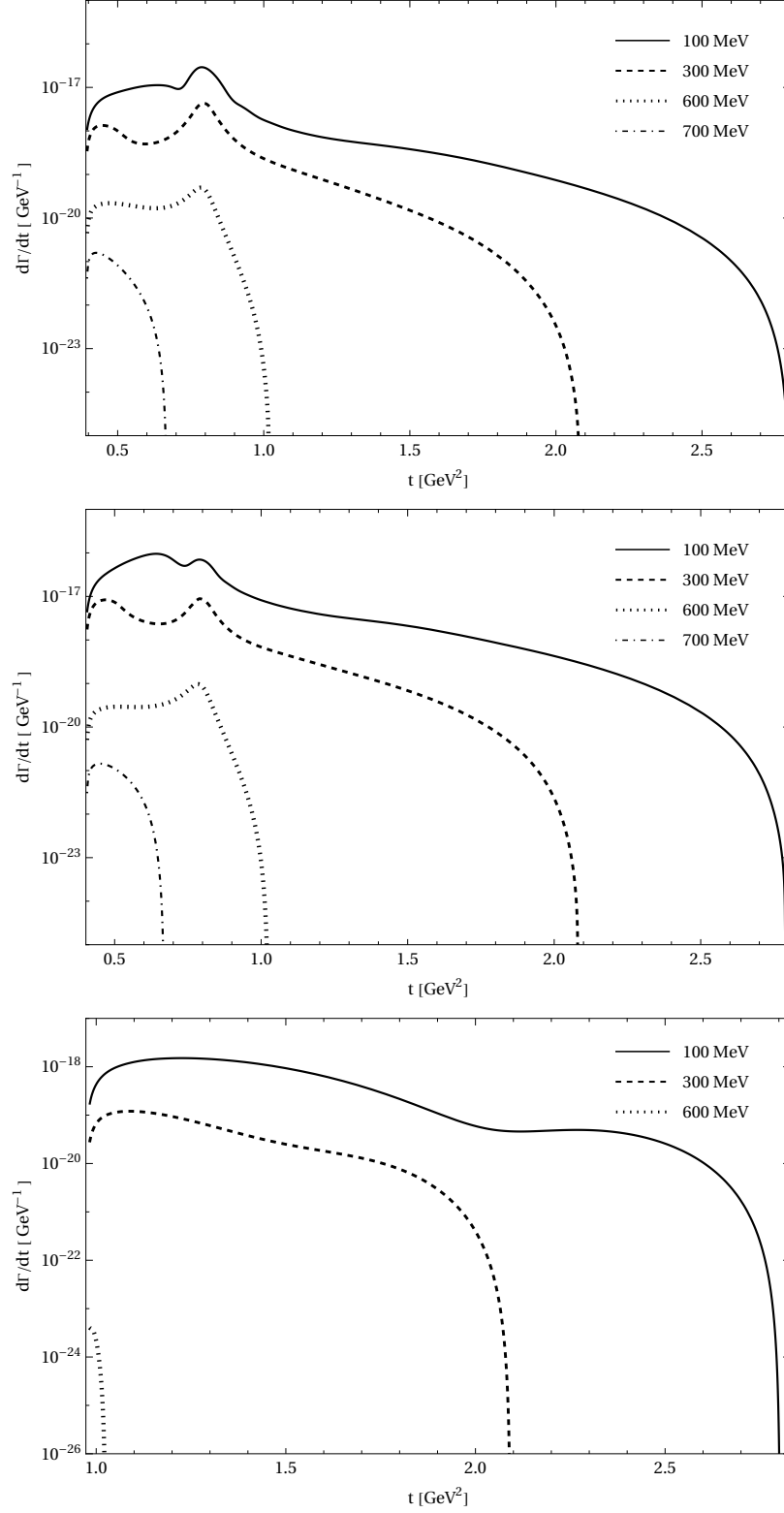


FIG. 7. The $K^- \pi^0$ (top), $\bar{K}^0 \pi^-$ (centre) and $K^- K^0$ (bottom) SI hadronic invariant mass distributions for several E_γ^{cut} values.

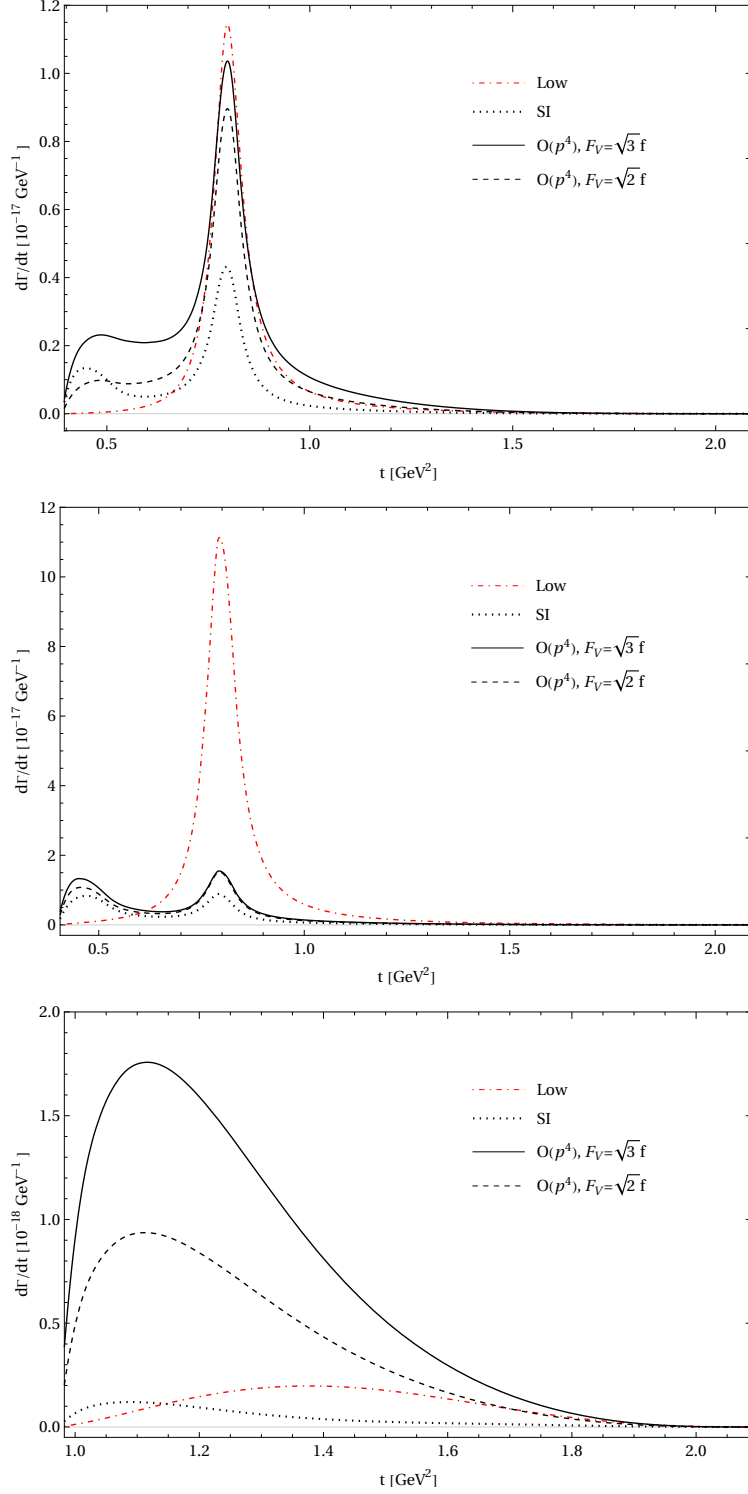


FIG. 8. The $K^- \pi^0$ (top), $\bar{K}^0 \pi^-$ (centre) and $K^- K^0$ (bottom) hadronic invariant mass distributions for $E_\gamma^{\text{cut}} \geq 300 \text{ MeV}$. The solid and dashed line represent the $\mathcal{O}(p^4)$ corrections using $F_V = \sqrt{3}F$ and $F_V = \sqrt{2}F$, respectively. The dotted line represents the bremsstrahlung contribution (SI). The red one corresponds to the Low approximation.

makes that in the case of the $K^- \pi^0$ mode these two leading subdominant contributions approximately cancel each other and the Low and full distributions are quite similar at the $K^*(892)$ peak. Conversely, for the $\bar{K}^0 \pi^-$ mode, the two contributions combine with the overall effect of decreasing considerably the peak. Finally, we just mention that the $K^- K^0$ invariant mass distribution is more sensitive to SD contributions, although the $\rho(1450)$ effect is hidden in the spectrum because of the corresponding kinematical suppression.

The photon energy distribution is shown in Fig. 9. The SI amplitude in all these decays governs the distribution for $E_\gamma \lesssim 100$ MeV, in agreement with the outcomes for the branching ratio. However, the SD contributions become relevant for $E_\gamma \gtrsim 250$ MeV. This feature makes these decays an excellent probe for testing SD effects. The same analysis for the $\tau^- \rightarrow \pi^- \pi^0 \nu_\tau \gamma$ decays can be found for instance in Ref. [53].

IV. RADIATIVE CORRECTIONS

The overall differential decay width is given by

$$\left. \frac{d\Gamma}{dt} \right|_{PP(\gamma)} = \left. \frac{d\Gamma}{dt} \right|_{PP} + \left. \frac{d\Gamma}{dt} \right|_{\text{III}} + \left. \frac{d\Gamma}{dt} \right|_{\text{IV/III}} + \left. \frac{d\Gamma}{dt} \right|_{\text{rest}}, \quad (31)$$

where the first term is the non-radiative differential width in Eq. (C5), the second and third terms correspond to the Low approximation integrated according to the kinematics in Refs. [51, 53], Eq. (15), and the last term includes the remaining contributions.

To evaluate the first term in the right-hand side of Eq. (31) we use two models for the factorization of the radiative corrections to the form factors. Both of them were pioneered in $K_{\ell 3}$ decays and have also been employed in the $\tau^- \rightarrow (K\pi)^- \nu_\tau$ processes. As we will see, the difference between both results will saturate the uncertainty of our real-photon radiative corrections. To the best of our knowledge, the importance of the factorization model for the former corrections was not previously recognized in the literature.

The contributions to the form factors due to virtual corrections can be written as

$$F_{+/0}(t, u) = F_{+/0}(t) + \delta F_{+/0}(t, u), \quad (32)$$

where $\delta F_0(t, u) = \delta F_+(t, u) + \frac{t}{\Delta_{-0}} \delta \bar{f}_-(u)$. In model 1, $\delta F_+(t, u)$ is given by [51]

$$\frac{\delta F_+(t, u)}{F_+(t)} = \frac{\alpha}{4\pi} \left[2(m_-^2 + m_\tau^2 - u) \mathcal{C}(u, M_\gamma) + 2 \log \left(\frac{m_- m_\tau}{M_\gamma^2} \right) \right] + \delta \bar{f}_+(u), \quad (33)$$

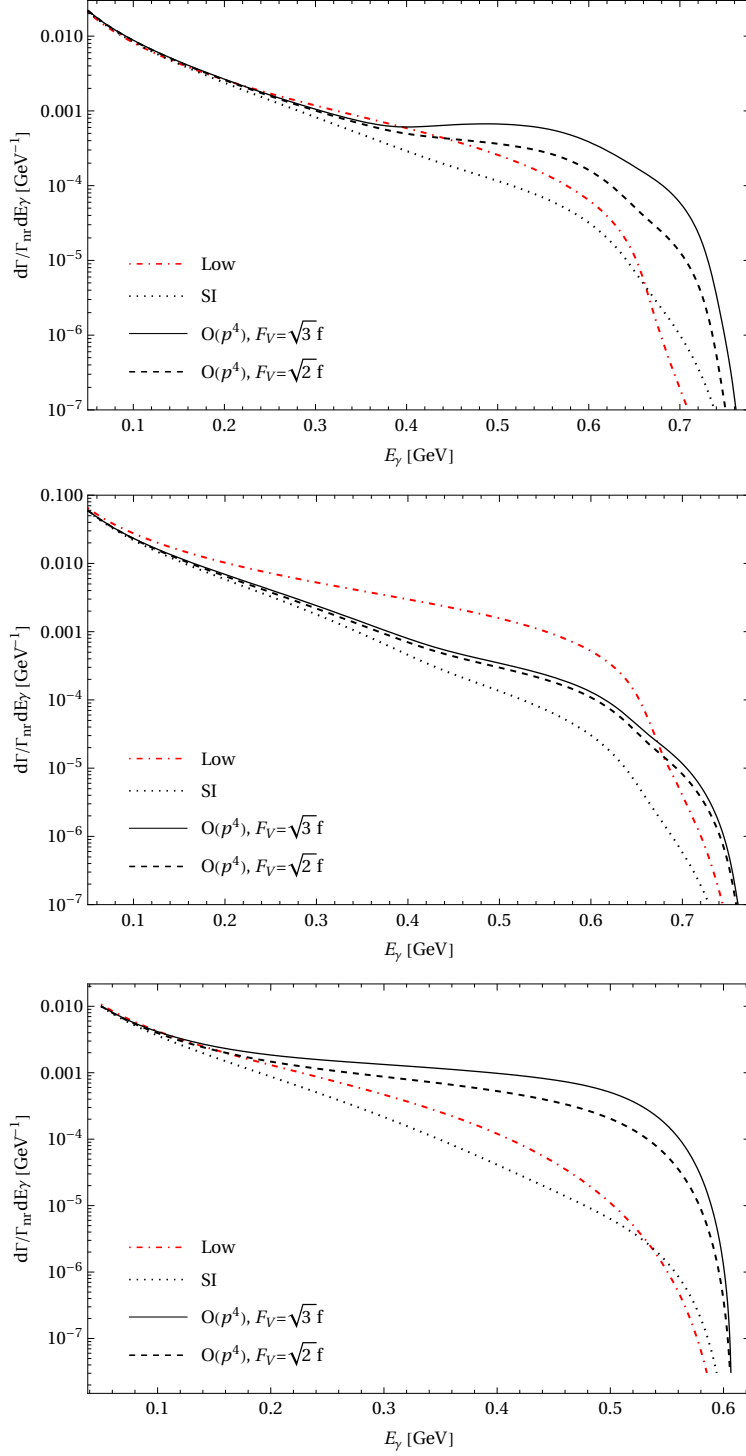


FIG. 9. Photon energy distribution for the $\tau^- \rightarrow K^- \pi^0 \nu_\tau \gamma$ (top), the $\tau^- \rightarrow \bar{K}^0 \pi^- \nu_\tau \gamma$ (centre) and the $\tau^- \rightarrow K^- K^0 \nu_\tau \gamma$ (bottom) decays normalized with the non-radiative decay width. The dotted line represents the bremsstrahlung contribution and the red one the Low approximation. The solid and dashed lines represent the $\mathcal{O}(p^4)$ corrections using $F_V = \sqrt{3}F$ and $F_V = \sqrt{2}F$, respectively.

while in model 2, it is written as [11] (we note that in this second case, the correction $\delta\bar{f}_+(u)$ to $\delta F_+(t, u)$ is not modulated by the vector form factor $F_+(t)$)

$$\frac{\delta F_+(t, u)}{F_+(t)} = \frac{\alpha}{4\pi} \left[2(m_-^2 + m_\tau^2 - u)\mathcal{C}(u, M_\gamma) + 2\log\left(\frac{m_- m_\tau}{M_\gamma^2}\right) \right] + \frac{\delta\bar{f}_+(u)}{F_+(t)}, \quad (34)$$

where $\mathcal{C}(u, M_\gamma)$, $\delta\bar{f}_+(u)$ and $\delta\bar{f}_-(u)$ are defined in App. B. A similar factorization prescription was used in Ref. [102], where model 2 was preferred over model 1 for the $K_{\mu 3}$ decays since the loop contributions to $\bar{f}_{+/-}(u)$ are different⁷. We will see here that model 1 factorization warrants smoother corrections than model 2 when resonance contributions are included, as resonance enhancements will cancel in the long-distance radiative correction factor $G_{\text{EM}}(t)$ in Eq. (35), as opposed to model 2. This motivates our preference of model 1 over model 2 in our following phenomenological analysis.

A couple of points are worth to stress in connection to both factorization models and the preferred one. First, a measurement of di-meson or photon energy spectra in the considered decays will be really helpful in reducing the model-dependence of our results (particularly on the factorization prescription). Second, we will present elsewhere the corresponding computations of the virtual photon structure-dependent corrections, which will complete these at the one-loop order. We expect that the model-dependence is reduced in the sum of all radiative corrections, so having this last missing piece available will also be valuable for diminishing the model-dependence (again with particular emphasis on the precise factorization in the considered decays).

The correction factors $\bar{\delta}_A(t)$ for the four-body decays and $\tilde{\delta}_A(t)$ for the three-body processes appearing in Eqs. (16) and (C6), respectively, where $A = +, 0, +0$, are both IR divergent when $M_\gamma \rightarrow 0$. Nevertheless, the overall contribution, $\delta_A(t) = \bar{\delta}_A(t) + \tilde{\delta}_A(t)$, is finite. In Fig. 10, we show the predictions for $\delta_A(t)$ for the $K^- \pi^0$, $\bar{K}^0 \pi^-$ and $K^- K^0$ decay modes using the form factors in model 1 and 2. Whilst our results for $\delta_+(t)$ in model 2 agree with those in Ref. [11] in Figure 2, the predictions for $\delta_0(t)$ are slightly different as a consequence of the parameterization of the scalar form factor⁸.

⁷ Both prescriptions were studied for the K_{e3} decays in Ref. [69], their outcomes for $\delta_{\text{EM}}^{K_\ell}(\mathcal{D}_3)(\%)$ are shifted from 0.41 to 0.56 for K_{e3}^0 and from -0.564 to -0.410 for K_{e3}^\pm modes where the former numbers correspond to model 2.

⁸ This effect is mainly responsible for the slight difference between our results for model 2 in Table 10 and those in Ref. [11].

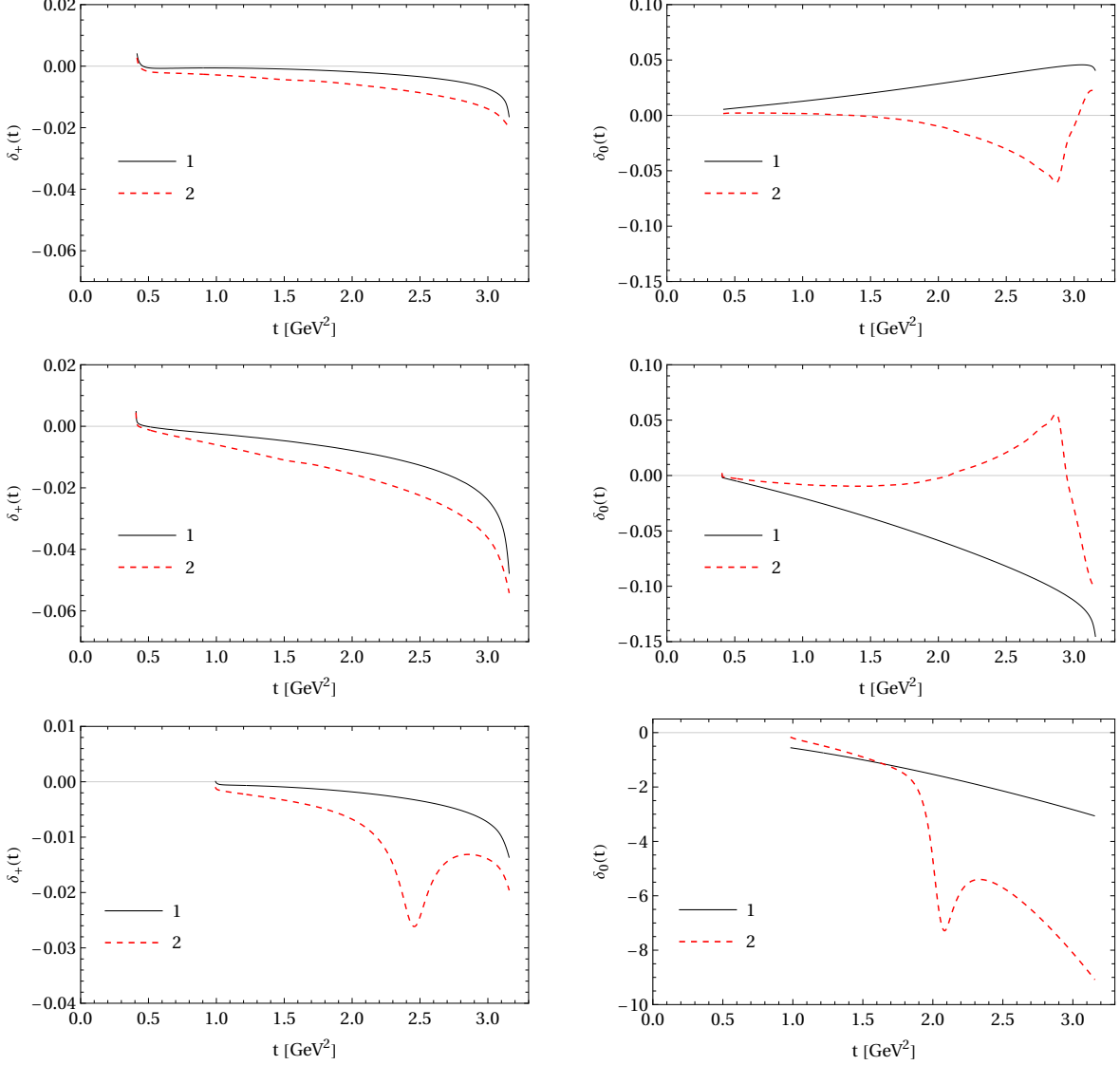


FIG. 10. Correction factors $\delta_+(t)$ (left) and $\delta_0(t)$ (right) to the differential decay rates of the $K^-\pi^0$, $\bar{K}^0\pi^-$ and K^-K^0 modes from top to bottom, according to models 1 (solid black) and 2 (dashed red).

The differential decay width can be written as

$$\begin{aligned}
 \left. \frac{d\Gamma}{dt} \right|_{PP(\gamma)} &= \frac{G_F^2 |V_{ud}F_+(0)|^2 S_{EW} m_\tau^3}{768\pi^3 t^3} \left(1 - \frac{t}{m_\tau^2}\right)^2 \lambda^{1/2}(t, m_-^2, m_0^2) \\
 &\times \left[C_V^2 |\tilde{F}_+(t)|^2 \left(1 + \frac{2t}{m_\tau^2}\right) \lambda(t, m_-^2, m_0^2) + 3C_S^2 \Delta_{-0}^2 |\tilde{F}_0(t)|^2 \right] G_{EM}(t),
 \end{aligned} \tag{35}$$

where $G_{EM}(t)$ encodes the electromagnetic corrections due to real and virtual photons. For simplicity, we have split $G_{EM}(t)$ in two parts: the leading Low approximation plus non-radiative contributions, $G_{EM}^{(0)}(t)$, and the remainder, $\delta G_{EM}(t)$, which includes the SD contributions to the

δ_{EM}^{PP}	Ref. [11]	$G_{\text{EM}}^{(0)}(t)$		$\delta G_{\text{EM}}(t)$		
		Model 1	Model 2	SI	SI + 2F	SI + 3F
$K^- \pi^0$	-0.20(20)	-0.019	-0.137	-0.001	+0.006	+0.010
$\bar{K}^0 \pi^-$	-0.15(20)	-0.086	-0.208	-0.098	-0.085	-0.080
$K^- K^0$	—	-0.046	-0.223	-0.012	+0.003	+0.016
$\pi^- \pi^0$	—	-0.196	-0.363	-0.010	-0.002	+0.010

TABLE IV. Electromagnetic corrections to hadronic τ decays in %.

amplitude. The predictions for both are shown in Fig. 11.

Integrating upon t , we get

$$\Gamma_{PP(\gamma)} = \frac{G_F^2 S_{\text{EW}} m_\tau^5}{96\pi^3} |V_{ud} F_+(0)|^2 I_{PP}^\tau (1 + \delta_{\text{EM}}^{PP})^2, \quad (36)$$

where

$$I_{PP}^\tau = \frac{1}{8m_\tau^2} \int_{t_{\text{thr}}}^{m_\tau^2} \frac{dt}{t^3} \left(1 - \frac{t}{m_\tau^2}\right)^2 \lambda^{1/2}(t, m_-^2, m_0^2) \times \left[C_V^2 |\tilde{F}_+(t)|^2 \left(1 + \frac{2t}{m_\tau^2}\right) \lambda(t, m_-^2, m_0^2) + 3C_S^2 \Delta_{-0}^2 |\tilde{F}_0(t)|^2 \right]. \quad (37)$$

The results for δ_{EM}^{PP} are shown in Table IV, where the third and fourth columns correspond to the sum of the first three terms in Eq. (31), and the last three columns to the fourth term in that equation. The value in model 1 for the $\bar{K}^0 \pi^-$ channel agrees with the result in Ref. [57], which is related to our definition by $\delta_{\text{EM}}^{\bar{K}^0 \pi^-} = \delta_{\text{EM}}^{\text{m.i.}}/2 \simeq -0.063\%$. Although our outcomes for the $(K\pi)^-$ modes agree within errors with those in Refs. [11, 57], the value in model 2 (and also model 1) for the $K^- \pi^0$ decay channel is larger than the $K^0 \pi^-$ one, which is at odds with Ref. [11]⁹.

The complete radiative corrections (that we always quote in %) are obtained adding to the model 1/2 results, which comprise the (negligible) $\mathcal{D}^{\text{IV/III}}$ part, the $2F/3F$ contributions, which include the SI part. We explained before why we prefer the model 1 over the model 2 results. We will take the difference with respect to model 2 as an asymmetric error on the model 1 results. For the structure-dependent contributions, we consider the $3F$ results as our central values and the difference with respect to $2F$ as a symmetric error for our model-dependence. To be on the safe side, we will take twice this error as our corresponding uncertainty. Finally, we have to account for the

⁹ Incidentally, our results would agree more closely swapping the numbers for $\delta_{\text{EM}}^{K^- \tau} \leftrightarrow \delta_{\text{EM}}^{\bar{K}^0 \tau}$ in Ref. [11].

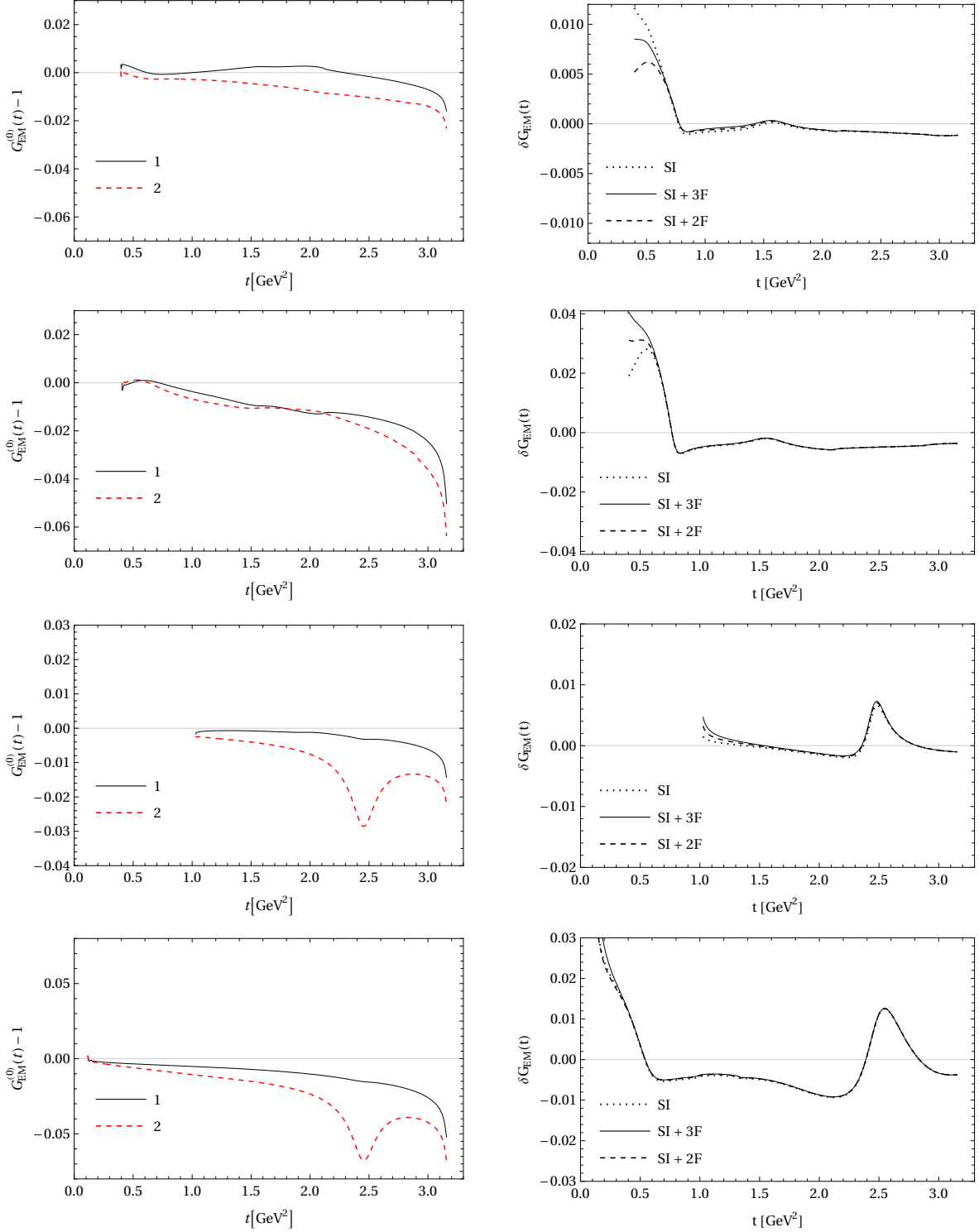


FIG. 11. Correction factors $G_{EM}^{(0)}(t) - 1$ (left) and $\delta G_{EM}(t)$ (right) to the differential decay rates of the $K^- \pi^0$, $\bar{K}^0 \pi^-$, $K^- K^0$, and $\pi^- \pi^0$ modes from top to bottom.

uncertainty associated to the missing structure-dependent virtual-photon corrections. According to the results in Refs. [43, 44] for the one-meson tau decays, this contribution is of the same size as the structure-independent correction. We will thus estimate its absolute value as the sum of the ‘Model 1’ and ‘SI+3F’ results in Table IV, allowing it to have either sign. We will assign an additional 60% uncertainty on it according to the results in Ref. [43, 44]. Proceeding this way, our main results are

$$\begin{aligned}\delta_{\text{EM}}^{K^-\pi^0} &= - (0.009_{-0.118}^{+0.010}) , & \delta_{\text{EM}}^{\bar{K}^0\pi^-} &= - (0.166_{-0.157}^{+0.100}) , \\ \delta_{\text{EM}}^{K^-K^0} &= - (0.030_{-0.180}^{+0.032}) , & \delta_{\text{EM}}^{\pi^-\pi^0} &= - (0.186_{-0.203}^{+0.114}) .\end{aligned}\tag{38}$$

We see that the model-independent contributions are responsible for the relatively large radiative corrections obtained for the $(\bar{K}/\pi)^0\pi^-$ modes. For the modes with a K^- , the dominant (asymmetric) uncertainty comes from the difference between the model 1/2 results, which is much larger than the deviation between the model-dependent $2F/3F$ values. Instead, for the modes with a π^- , the dominant uncertainty comes from the missing model-dependent virtual-photon corrections. Our results for the $\delta_{\text{EM}}^{K^-\pi^0/\bar{K}^0\pi^-}$ agree with those in Ref. [11], and we reduce the uncertainty band by $\sim 45\%$ in the K^- channel. We note that the estimate of the errors in this reference yields also an uncertainty band in agreement with ours for $\delta_{\text{EM}}^{K^-K^0/\pi^-\pi^0}$ (our errors are smaller by a factor ~ 2 again in the K^-K^0 case) ¹⁰. Although our $\delta_{\text{EM}}^{K^-\pi^0}$ and $\delta_{\text{EM}}^{\bar{K}^0\pi^-}$ seem to differ (the main reason being the scaling of the inner bremsstrahlung contribution with the inverse of the charged meson mass), the corresponding significance of their non-equality is only $\sim 0.7\sigma$, according to our uncertainties. Our radiative corrections in Eq. (38) improve over previous analysis (where, for instance, the structure-dependent corrections were not computed) and, as such, should be employed in precision analysis like, e.g., CKM unitarity or lepton universality tests [103] and searches for non-standard interactions.

For completeness, we have also evaluated these corrections for the $K^-\eta^{(\prime)}$ modes. In the $G_{\text{EM}}^{(0)}$ approximation and using the respective dominance of the vector (scalar) form factor [13], we obtain

$$\delta_{\text{EM}}^{K^-\eta} = - (0.026_{-0.163}^{+0.029}) , \quad \delta_{\text{EM}}^{K^-\eta'} = - (0.304_{-0.185}^{+0.422}) ,\tag{39}$$

where the uncertainty is saturated by the difference between the model 1/2 results in the η channel and by the non yet computed virtual-photon structure-dependent corrections for the η' mode. The

¹⁰ A former estimation of the $\pi^-\pi^0$ radiative corrections yielded $\delta_{\text{EM}}^{\pi^-\pi^0} \sim -0.08\%$ [52], where the SD contributions were evaluated using a vector meson dominance model.

$K^- \eta'$ decay mode is the only one (completely) dominated by the scalar form factor, which causes the relatively large magnitude of the corresponding radiative correction.

V. IMPACT OF RADIATIVE CORRECTIONS ON NP BOUNDS

In this section, we update the results of Ref. [41] concerning one- and two-meson tau decays including the radiative corrections computed in this paper ¹¹. We recall briefly the main aspects here, but refer the reader to Ref. [41] for details.

The low-energy effective Lagrangian describing the $\tau^- \rightarrow \bar{u} D \nu_\tau$ decays ($D = d, s$) can be written as [104, 105]

$$\begin{aligned} \mathcal{L}_{\text{eff}} = & -\frac{G_F V_{ud}}{\sqrt{2}} \left[(1 + \varepsilon_L^\tau) \bar{\tau} \gamma_\mu (1 - \gamma_5) \nu_\tau \cdot \bar{u} \gamma^\mu (1 - \gamma_5) D + \varepsilon_R^\tau \bar{\tau} \gamma_\mu (1 - \gamma_5) \nu_\tau \cdot \bar{u} \gamma^\mu (1 + \gamma_5) D \right. \\ & \left. + \bar{\tau} (1 - \gamma_5) \nu_\tau \cdot \bar{u} (\varepsilon_S^\tau - \varepsilon_P^\tau \gamma_5) D + \varepsilon_T^\tau \bar{\tau} \sigma_{\mu\nu} (1 - \gamma_5) \nu_\tau \cdot \bar{u} \sigma^{\mu\nu} (1 - \gamma_5) D \right] + \text{h.c.} , \end{aligned} \quad (40)$$

where G_F corresponds to the Standard Model (SM) tree-level definition of the Fermi constant and the non-vanishing ε_i ($i = S, P, V, A, T$) Wilson coefficients (assumed to be real for simplicity in what follows) determine the new physics. Beyond the SM, super allowed nuclear Fermi β decays do not depend on $G_F V_{ud}$ but rather on $G_F V_{ud} (1 + \varepsilon_L^e + \varepsilon_R^e)$, as it is accounted for in our analysis. After using \mathcal{L}_{eff} , the relevant (for two-meson decays) scalar, vector and tensor hadron matrix elements are computed using dispersion relations, nourished with experimental data, keeping track of the associated uncertainties.

We will discuss in the following the separate results for the strangeness-conserving and changing channels and, finally, those of a joint fit.

A. $\Delta S = 0$

From $\tau^- \rightarrow \pi^- \nu_\tau(\gamma)$, we restrict [37, 41, 43, 44, 46]

$$\varepsilon_L^\tau - \varepsilon_L^e - \varepsilon_R^\tau - \varepsilon_R^e - \frac{m_\pi^2}{m_\tau(m_u + m_d)} \varepsilon_P^\tau = -(0.14 \pm 0.72) \cdot 10^{-2} , \quad (41)$$

using $f_\pi = 130.2(8) \text{ MeV}$ [3], $|V_{ud}| = 0.97373(31)$ [92], $S_{\text{EW}} = 1.0232$ [65], masses and branching ratios from the PDG [92], and $\delta_{\text{em}}^{\tau\pi} = -0.24(56)\%$ from Ref. [44].

¹¹ One-meson channels were updated in Refs. [43, 44] using the improved radiative corrections calculated in those papers. It would also be interesting to reanalyse Refs. [11, 46] with our new radiative corrections.

After performing a fit that includes one (π) and two meson ($\pi\pi$, KK) strangeness-conserving exclusive tau decays, the constraints for the non-standard interactions (at $\mu = 2$ GeV in the $\overline{\text{MS}}$ scheme) are

$$\begin{pmatrix} \varepsilon_L^\tau - \varepsilon_L^e + \varepsilon_R^\tau - \varepsilon_R^e \\ \varepsilon_R^\tau + \frac{m_\pi^2}{2m_\tau(m_u+m_d)} \varepsilon_P^\tau \\ \varepsilon_S^\tau \\ \varepsilon_T^\tau \end{pmatrix} = \begin{pmatrix} 0.0 \pm 0.6 \begin{smallmatrix} +6.8 \\ -6.4 \end{smallmatrix} \pm 0.1 \pm 1.7 \begin{smallmatrix} +0.0 \\ -0.2 \end{smallmatrix} \\ 0.1 \pm 0.5 \begin{smallmatrix} +3.4 \\ -3.3 \end{smallmatrix} \pm 0.1 \pm 0.9 \pm 0.1 \\ 10.3 \pm 0.5 \begin{smallmatrix} +1.2 \\ -25.0 \end{smallmatrix} \pm 0.1 \pm 0.9 \begin{smallmatrix} +6.2 \\ -22.4 \end{smallmatrix} \\ 0.4 \pm 0.2 \begin{smallmatrix} +4.1 \\ -4.4 \end{smallmatrix} \pm 0.1 \pm 1.1 \begin{smallmatrix} +0.3 \\ -0.2 \end{smallmatrix} \end{pmatrix} \times 10^{-2}, \quad (42)$$

with $\chi^2/\text{dof} \sim 0.8$, and the associated (statistical) correlation matrix is

$$\rho_{ij} = \begin{pmatrix} 1 & 0.662 & -0.487 & -0.544 \\ & 1 & -0.323 & -0.360 \\ & & 1 & 0.452 \\ & & & 1 \end{pmatrix}. \quad (43)$$

The first error in Eq. (42) is the statistical fit uncertainty, the second error comes from the theoretical uncertainty associated to the pion form factor, the third and fourth ones come from the quark masses and from the uncertainty related to the tensor form factor, respectively, and the last error is a systematic uncertainty coming from the radiative corrections to two-meson tau decays.

The results obtained are extremely consistent with those in Ref. [41]. In general, the uncertainties induced by the radiative corrections are negligible with respect to others except for ε_S^τ , where they are leading. This is interesting since this is the largest Wilson coefficient, so its compatibility with the SM gets even stronger upon including our new radiative corrections computed in this work.

B. $|\Delta S| = 1$

From $\tau^- \rightarrow K^- \nu_\tau$, we bind [37, 41, 43, 44, 46]

$$\varepsilon_L^\tau - \varepsilon_L^e - \varepsilon_R^\tau - \varepsilon_R^e - \frac{m_K^2}{m_\tau(m_u+m_s)} \varepsilon_P^\tau = -(1.02 \pm 0.86) \cdot 10^{-2}, \quad (44)$$

using the lattice result $f_K = 155.7(3)$ MeV [3], $|V_{us}| = 0.2243(8)$ [92], masses and branching ratios from PDG [92], and $\delta_{\text{em}}^{\tau K} = -0.15(57)\%$ from Ref. [44].

The bounds for the non-SM effective couplings resulting from a fit to one (K) and two meson ($K\pi, K\eta$) strangeness-changing transitions (at $\mu = 2$ GeV in the $\overline{\text{MS}}$ scheme) are

$$\begin{pmatrix} \varepsilon_L^\tau - \varepsilon_L^\rho + \varepsilon_R^\tau - \varepsilon_R^\rho \\ \varepsilon_R^\tau + \frac{m_K^2}{2m_\tau(m_u+m_s)}\varepsilon_P^\tau \\ \varepsilon_S^\tau \\ \varepsilon_T^\tau \end{pmatrix} = \begin{pmatrix} 0.4 \pm 1.5 \pm 0.4 \begin{smallmatrix} +0.1 \\ -0.0 \end{smallmatrix} \\ 0.7 \pm 0.9 \pm 0.2 \begin{smallmatrix} +0.1 \\ -0.0 \end{smallmatrix} \\ 0.8 \pm 0.9 \pm 0.2 \begin{smallmatrix} +0.0 \\ -0.1 \end{smallmatrix} \\ 0.5 \pm 0.7 \pm 0.4 \pm 0.0 \end{pmatrix} \times 10^{-2}, \quad (45)$$

with $\chi^2/\text{dof} \sim 0.9$, and

$$\rho_{ij} = \begin{pmatrix} 1 & 0.874 & -0.149 & 0.463 \\ & 1 & -0.130 & 0.404 \\ & & 1 & -0.057 \\ & & & 1 \end{pmatrix}. \quad (46)$$

In this case, the first error in Eq. (45) is the statistical fit uncertainty, the second one is due to the tensor form factor, and the last uncertainty is associated to the radiative corrections to two-meson tau decays. The uncertainties related to the kaon vector form factor and the quark masses are negligible. These results comply nicely with those in Ref. [41], and the uncertainty induced by the radiative corrections is in all couplings negligible.

C. $\Delta S = 0$ and $|\Delta S| = 1$ joint fit

Our previous fits to the strangeness-conserving and changing channels were not able to separate ε_R^τ and ε_P^τ ¹². In Ref. [41], we attained this within Minimal Flavour Violation [106] (MFV)¹³, as we will do here. The CKM matrix elements used in this analysis are obtained from the correlation between $|V_{ud}|$ and $|V_{us}|$, $|V_{us}/V_{ud}| = 0.2313(5)$, and $|V_{us}| = 0.2232(6)$ from Ref. [3], which correspond to the region described by the red ellipse in Fig. 10 of Ref. [3].

Performing thus a joint fit that includes both one and two meson strangeness-conserving and strangeness-changing tau decays (within MFV), the limits for the NP effective couplings (at $\mu =$

¹² This was achieved by combining inclusive and exclusive information in Refs. [37, 46].

¹³ MFV assumes that flavour mixing within the Standard Model Effective Field Theory (SMEFT) is aligned with the SM one (here, in particular, in the quark sector). This generally allows for orders of magnitude smaller new physics scales in precision flavour tests.

2 GeV in the $\overline{\text{MS}}$ scheme) are

$$\begin{pmatrix} \varepsilon_L^\tau - \varepsilon_L^e + \varepsilon_R^\tau - \varepsilon_R^e \\ \varepsilon_R^\tau \\ \varepsilon_P^\tau \\ \varepsilon_S^\tau \\ \varepsilon_T^\tau \end{pmatrix} = \begin{pmatrix} 2.7 \pm 0.5 \begin{smallmatrix} +2.3 \\ -3.1 \end{smallmatrix} \pm 0.4 \begin{smallmatrix} +0.4 \\ -0.5 \end{smallmatrix} \pm 0.0 \pm 0.3 \begin{smallmatrix} +0.0 \\ -1.3 \end{smallmatrix} \pm 0.0 \\ 7.1 \pm 4.7 \begin{smallmatrix} +1.2 \\ -1.6 \end{smallmatrix} \pm 0.9 \pm 1.8 \pm 0.2 \begin{smallmatrix} +12.3 \\ -3.6 \end{smallmatrix} \pm 0.0 \\ -7.7 \pm 6.1 \pm 0.0 \begin{smallmatrix} +1.3 \\ -1.2 \end{smallmatrix} \begin{smallmatrix} +2.4 \\ -2.3 \end{smallmatrix} \pm 0.0 \begin{smallmatrix} +4.1 \\ -17.0 \end{smallmatrix} \pm 0.0 \\ 5.3 \begin{smallmatrix} +0.6 \\ -0.7 \end{smallmatrix} \begin{smallmatrix} +2.0 \\ -14.9 \end{smallmatrix} \begin{smallmatrix} +0.1 \\ -0.0 \end{smallmatrix} \pm 0.0 \pm 0.1 \begin{smallmatrix} +0.1 \\ -15.9 \end{smallmatrix} \begin{smallmatrix} +0.1 \\ -0.0 \end{smallmatrix} \\ -0.2 \pm 0.2 \begin{smallmatrix} +3.6 \\ -2.9 \end{smallmatrix} \begin{smallmatrix} +0.1 \\ -0.0 \end{smallmatrix} \pm 0.0 \pm 0.4 \begin{smallmatrix} +0.5 \\ -0.0 \end{smallmatrix} \begin{smallmatrix} +0.2 \\ -0.0 \end{smallmatrix} \end{pmatrix} \times 10^{-2}, \quad (47)$$

with $\chi^2/\text{dof} \sim 1.5$, and

$$\rho_{ij} = \begin{pmatrix} 1 & 0.056 & 0.000 & -0.270 & -0.402 \\ & 1 & -0.997 & -0.015 & -0.023 \\ & & 1 & 0.000 & 0.000 \\ & & & 1 & 0.235 \\ & & & & 1 \end{pmatrix}. \quad (48)$$

Now, the first error in Eq. (47) corresponds again to the statistical fit uncertainty, the second one comes from the uncertainty on the pion form factor, the third error is related to the CKM matrix elements $|V_{ud}|$ and $|V_{us}|$, the fourth one comes from the radiative corrections $\delta_{\text{em}}^{\tau\pi}$ and $\delta_{\text{em}}^{\tau K}$, the fifth error is associated to the tensor form factor, the sixth error comes from the uncertainty of the quark masses, and the last one is due to the radiative corrections to two-meson tau decays.

These results accord with Ref. [41] closely. As seen, in this joint fit the uncertainties induced by radiative corrections are always subdominant.

VI. CONCLUSIONS

Radiative corrections to the one-meson tau decays have been employed in CKM unitarity, lepton universality and non-standard interactions tests. The corresponding results for the di-pion tau decays allowed tau-based computations of the leading-order piece of the hadronic vacuum polarization part of the muon $g - 2$. Even though the model-independent part of these corrections was available for the $K\pi$ modes, the structure-dependent one remained to be calculated. We have performed the first step towards bridging this gap, by computing the real-photon structure-dependent radiative correction factors with reduced uncertainties, and will continue with the required virtual-photon model-dependent corrections in a forthcoming work. For completeness, we also quoted our numbers for the PP ($P = \pi, K$) modes and estimated them for the $K\eta^{(\prime)}$ cases.

We recapitulate our main results in Eq. (38):

$$\begin{aligned}\delta_{\text{EM}}^{K^-\pi^0} &= - (0.009_{-0.118}^{+0.010}) \% , & \delta_{\text{EM}}^{\bar{K}^0\pi^-} &= - (0.166_{-0.157}^{+0.100}) \% , \\ \delta_{\text{EM}}^{K^-K^0} &= - (0.030_{-0.180}^{+0.032}) \% , & \delta_{\text{EM}}^{\pi^-\pi^0} &= - (0.186_{-0.203}^{+0.114}) \% ,\end{aligned}$$

which reduce previous uncertainties by a factor of ~ 2 for the K^- modes and have similar errors to those quoted for the $\bar{K}^0\pi^-$ channel.

We have put forward the importance of the factorization model for the radiative corrections, which saturates the uncertainties in Eq. (38) for the K^- channels. Analogous relevance shall be found in the radiative corrections for processes including diverse final states with hadrons (if the resonance regime is allowed by phase space), which calls for further devoted studies. While lattice QCD obtains these complicated radiative corrections, a deeper understanding of their factorization will probe key in increasing the reach of new physics searches through processes including hadrons.

We have finally illustrated the application of our results updating our fits of non-SM interactions in di-meson tau decays (also one-meson channels were included in the fits), finding results compatible with our earlier work, where these corrections and their uncertainties were neglected. As interesting outlooks, the reanalysis of Refs. [36, 38] (looking for NP in $\tau^- \rightarrow \pi^- \pi^0 \nu_\tau$ and $\tau^- \rightarrow (K\pi)^- \nu_\tau$ decays, respectively), of inclusive and exclusive semileptonic tau decays[37, 46] and of the impact of kaon data on strangeness-violating tau decays [11], are among the important applications of our results that we can envisage, which can be incorporated into the HFLAV analysis [107]. All these studies will benefit from our future results for the virtual-photon structure-dependent radiative corrections.

ACKNOWLEDGMENTS

The work of R. E. has been supported by the European Union's Horizon 2020 Research and Innovation Programme under grant 824093 (H2020-INFRAIA- 2018-1), the Ministerio de Ciencia e Innovación under grant PID2020-112965GB-I00, and by the Departament de Recerca i Universitats from Generalitat de Catalunya to the Grup de Recerca 'Grup de Física Teòrica UAB/IFAE' (Codi: 2021 SGR 00649). IFAE is partially funded by the CERCA program of the Generalitat de Catalunya. J. A. M. is also supported by MICINN with funding from European Union NextGenerationEU (PRTR-C17.I1) and acknowledges Conacyt for his PhD scholarship. P. R. was partly

funded by Conacyt's project within 'Paradigmas y Controversias de la Ciencia 2022', number 319395, and by Cátedra Marcos Moshinsky (Fundación Marcos Moshinsky) 2020.

Appendix A: $K_{\ell 3}$ decays

The most general amplitude for the $K(p_K) \rightarrow \pi(p_\pi)\ell(P)v_\ell(q')\gamma(k)$ decays that complies with Lorentz invariance and the discrete symmetries of QCD can be written as

$$\begin{aligned} \mathcal{M} = & \frac{eG_F V_{us}^*}{\sqrt{2}} \varepsilon_\mu^* \left[\frac{H_V(-p_K, p_\pi)}{k^2 + 2k \cdot P} \bar{u}(q') \gamma^\nu (1 - \gamma^5) (m_\ell - \not{P} - \not{k}) \gamma^\mu v(P) \right. \\ & \left. + (V^{\mu\nu} - A^{\mu\nu}) \bar{u}(q') \gamma_\nu (1 - \gamma^5) v(P) \right], \end{aligned} \quad (\text{A1})$$

where

$$\begin{aligned} H^V(-p_K, p_\pi) & \equiv \langle \pi(p_\pi) | \bar{s} \gamma^\nu u | K(p_K) \rangle \\ & = -C_V F_+(t) \left[(p_K + p_\pi)^\nu - \frac{\Delta_{K\pi}}{t} (p_K - p_\pi)^\nu \right] - C_S \frac{\Delta_{K\pi}}{t} (p_K - p_\pi)^\nu F_0(t), \end{aligned} \quad (\text{A2})$$

with $t = (p_K - p_\pi)^2$.

The structure-independent term is given by

$$\begin{aligned} V_{\text{SI}}^{\mu\nu} = & \frac{H^V(-p_K + k, p_\pi)(k - 2p_K)^\mu}{k^2 - 2k \cdot p_K} + \left\{ -C_V F_+(t') - \frac{\Delta_{K\pi}}{t'} [C_S F_0(t') - C_V F_+(t')] \right\} g^{\mu\nu} \\ & + C_V \frac{F_+(t') - F_+(t)}{k \cdot (p_K - p_\pi)} \left[(p_K + p_\pi)^\nu - \frac{\Delta_{K\pi}}{t} (p_K - p_\pi)^\nu \right] (p_K - p_\pi)^\mu \\ & + \frac{\Delta_{K\pi}}{t t'} \left\{ 2 [C_S F_0(t') - C_V F_+(t')] + \frac{C_S t'}{k \cdot (p_K - p_\pi)} [F_0(t') - F_0(t)] \right\} \\ & \times (p_K - p_\pi)^\mu (p_K - p_\pi)^\nu, \end{aligned} \quad (\text{A3})$$

where $C_V^{K^- \pi^0} = C_S^{K^- \pi^0} = 1/\sqrt{2}$ for $K^+ \rightarrow \pi^0 \ell^+ v_\ell \gamma$, and

$$\begin{aligned} V_{\text{SI}}^{\mu\nu} = & \frac{H^V(-p_K, p_\pi + k)(k + 2p_\pi)^\mu}{k^2 + 2k \cdot p_\pi} + \left\{ C_V F_+(t') - \frac{\Delta_{K\pi}}{t'} [C_S F_0(t') - C_V F_+(t')] \right\} g^{\mu\nu} \\ & + C_V \frac{F_+(t') - F_+(t)}{k \cdot (p_K - p_\pi)} \left[(p_K + p_\pi)^\nu - \frac{\Delta_{K\pi}}{t} (p_K - p_\pi)^\nu \right] (p_K - p_\pi)^\mu \\ & + \frac{\Delta_{K\pi}}{t t'} \left\{ 2 [C_S F_0(t') - C_V F_+(t')] + \frac{C_S t'}{k \cdot (p_K - p_\pi)} [F_0(t') - F_0(t)] \right\} \\ & \times (p_K - p_\pi)^\mu (p_K - p_\pi)^\nu, \end{aligned} \quad (\text{A4})$$

where $C_V^{\bar{K}^0\pi^-} = C_S^{\bar{K}^0\pi^-} = 1$ for $K^0 \rightarrow \pi^- \ell^+ \nu_\ell \gamma$, both with $t' \equiv (p_K - p_\pi - k)^2$. All these expressions are obtained from Eqs. (1)–(3) by replacing $\{p_0^-\} \rightarrow \{p_\pi^-\}$, $\Delta_{-0} \rightarrow \Delta_{K\pi}$, $P \rightarrow -P$ and $m_\tau \rightarrow m_\ell$ for $K^+ \rightarrow \pi^0 \ell^+ \nu_\ell \gamma$, and $\{p_0^-\} \rightarrow \{p_\pi^-\}$, $\Delta_{-0} \rightarrow -\Delta_{K\pi}$, $C_{V,S} \rightarrow -C_{V,S}$, $P \rightarrow -P$ and $m_\tau \rightarrow m_\ell$ for $K^0 \rightarrow \pi^- \ell^+ \nu_\ell \gamma$. The structure-dependent terms are analogous to those in Eqs. (4) and (5).

At $\mathcal{O}(p^0)$, we get

$$V_{\text{SI}}^{\mu\nu} = -C_{K^+} \frac{p_K^\mu}{k \cdot p_K} (p_K + p_\pi)^\nu - C_{K^+} \left(g^{\mu\nu} - \frac{p_K^\mu k^\nu}{k \cdot p_K} \right), \quad (\text{A5})$$

for $K^+ \rightarrow \pi^0$, and

$$V_{\text{SI}}^{\mu\nu} = -C_{K^0} \frac{p_\pi^\mu}{k \cdot p_\pi} (p_K + p_\pi)^\nu + C_{K^0} \left(g^{\mu\nu} - \frac{p_\pi^\mu k^\nu}{k \cdot p_\pi} \right), \quad (\text{A6})$$

for $K^0 \rightarrow \pi^-$, where $C_K = C_S = C_V$. Thus, the overall amplitude at $\mathcal{O}(p^0)$ is given by

$$\mathcal{M}_\gamma = \frac{eG_F}{\sqrt{2}} V_{us}^* C_{K^+} \bar{u}(q') (1 + \gamma^5) (2\not{p}_\pi - m_\ell) \left(\frac{\varepsilon \cdot P}{k \cdot P} - \frac{\varepsilon \cdot p_K}{k \cdot p_K} + \frac{\not{k}\not{\varepsilon}}{2k \cdot P} \right) \nu(P), \quad (\text{A7})$$

and

$$\mathcal{M}_\gamma = \frac{eG_F}{\sqrt{2}} V_{us}^* C_{K^0} \bar{u}(q') (1 + \gamma^5) (2\not{p}_K + m_\ell) \left(\frac{\varepsilon \cdot P}{k \cdot P} - \frac{\varepsilon \cdot p_\pi}{k \cdot p_\pi} + \frac{\not{k}\not{\varepsilon}}{2k \cdot P} \right) \nu(P), \quad (\text{A8})$$

respectively. These two expressions agree with the Eqs. (13) and (14) in Ref. [69]. To this order, $V_{\text{SD}}^{\mu\nu}$ and $A_{\text{SD}}^{\mu\nu}$, which are $\mathcal{O}(p^2)$, can be neglected.

In the Low limit, we obtain

$$\mathcal{M}_\gamma = \frac{eG_F V_{us}^*}{\sqrt{2}} \bar{u}(q') \gamma_\nu (1 - \gamma^5) \nu(P) H^\nu(-p_K, p_\pi) \left(\frac{\varepsilon \cdot p_+}{k \cdot p_+} - \frac{\varepsilon \cdot P}{k \cdot P} \right), \quad (\text{A9})$$

where the subscript ‘+’ refers to the charged meson. The spin-averaged squared matrix element is then given by

$$\begin{aligned} \overline{|\mathcal{M}_\gamma|^2} &= 4C_K^2 e^2 G_F^2 |V_{us}|^2 S_{\text{EW}}^K \left\{ \left[\frac{m_\ell^2}{2} (t - m_\ell^2) + 2m_K^2 m_\pi^2 + 2u(m_\ell^2 - t + m_K^2 + m_\pi^2) - 2u^2 \right. \right. \\ &\quad \left. \left. - \frac{\Delta_{K\pi}}{t} m_\ell^2 (2u + t - m_\ell^2 - 2m_\pi^2) + \frac{\Delta_{K\pi}^2}{t^2} \frac{m_\ell^2}{2} (t - m_\ell^2) \right] |F_+(t)|^2 \right. \\ &\quad \left. + \frac{\Delta_{K\pi} m_\ell^2}{t} \left[2u + t - m_\ell^2 - 2m_\pi^2 + \frac{\Delta_{K\pi}}{t} (m_\ell^2 - t) \right] \text{Re}[F_+(t)F_0^*(t)] \right. \\ &\quad \left. + \frac{\Delta_{K\pi}^2 m_\ell^2}{2t^2} (t - m_\ell^2) |F_0(t)|^2 \right\} \sum_{\gamma \text{ pols.}} \left| \frac{p_- \cdot \varepsilon}{p_- \cdot k} - \frac{P \cdot \varepsilon}{P \cdot k} \right|^2 + \mathcal{O}(k^0), \end{aligned} \quad (\text{A10})$$

where $u = (p_K - P)^2$. The last expression can also be written in terms of $f_{+/-}(t)$,

$$\overline{|\mathcal{M}_\gamma|^2} = 2C_K^2 m_K^4 e^2 G_F^2 |V_{us}|^2 S_{\text{EW}}^K \rho^{(0)}(y, z) \sum_{\gamma \text{ pols.}} \left| \frac{p_- \cdot \varepsilon}{p_- \cdot k} - \frac{P \cdot \varepsilon}{P \cdot k} \right|^2 + \mathcal{O}(k^0), \quad (\text{A11})$$

where

$$\rho^{(0)}(y, z) = A_1^{(0)}(y, z) |f_+(t)|^2 + A_2^{(0)}(y, z) \text{Re} [f_+(t) f_-^*(t)] + A_3^{(0)}(y, z) |f_-(t)|^2, \quad (\text{A12})$$

and the kinematical densities are

$$A_1^{(0)} = 4(y + z - 1)(1 - y) + r_\ell(4y + 3z - 3) - 4r_\pi + r_\ell(r_\pi - r_\ell), \quad (\text{A13a})$$

$$A_2^{(0)} = 2r_\ell(r_\ell - r_\pi - 2y - z + 3), \quad (\text{A13b})$$

$$A_3^{(0)} = r_\ell(r_\pi - r_\ell + 1 - z), \quad (\text{A13c})$$

with

$$z = \frac{2p_\pi \cdot p_K}{m_K^2} = \frac{2E_\pi}{m_K}, \quad y = \frac{2p_K \cdot p_\ell}{m_K^2} = \frac{2E_\ell}{m_K}, \quad (\text{A14})$$

$r_\ell = (m_\ell/m_K)^2$, and $r_\pi = (m_\pi/m_K)^2$. Here, E_π (E_ℓ) is the energy of the pion (charged lepton) in the kaon rest frame. The expression in Eq. (A11) can be compared directly with the results in Refs. [69, 102, 108].

The $K \rightarrow \pi \ell \nu_\ell$ decay width without radiative corrections [11] is given by

$$\Gamma(K \rightarrow \pi \ell \nu_\ell) = \frac{G_F^2 m_K^5}{192 \pi^3} S_{\text{EW}}^K |V_{us}|^2 |F_+(0)| I_K^\ell, \quad (\text{A15})$$

where

$$I_K^\ell = \int_{m_\ell^2}^{t_{\text{max}}} dt \frac{1}{m_K^8} \lambda^{3/2}(t, m_K^2, m_\pi^2) \left(1 - \frac{m_\ell^2}{t}\right)^2 \left(1 + \frac{m_\ell^2}{2t}\right) \times \left[C_V^2 |\tilde{F}_+(t)|^2 + \frac{3\Delta_{K\pi}^2 m_\ell^2}{(2t + m_\ell^2) \lambda(t, m_K^2, m_\pi^2)} C_S |\tilde{F}_0(t)|^2 \right], \quad (\text{A16})$$

and $t_{\text{max}} = (m_K - m_\pi)^2$.

Appendix B: Virtual corrections to the hadronic tau decays

The radiative corrections to the $\tau^- \rightarrow (P_1 P_2)^- \nu_\tau$ decays at $\mathcal{O}(p^2)$ in ChPT [71–73] are depicted in Fig. 12. The overall contribution is given by [50]

$$\frac{\delta H^\mu(t, u)}{C_V} = \delta f_+(u) (p_1 - p_0)^\mu + \delta f_-(u) (p_1 + p_0)^\mu, \quad (\text{B1})$$

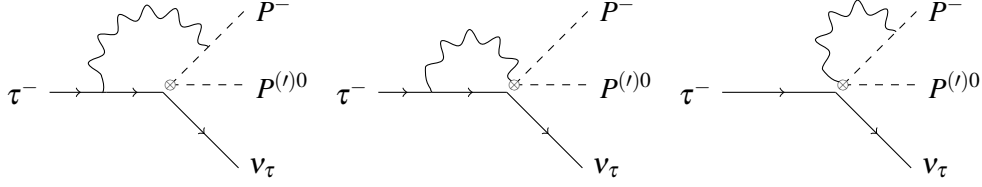


FIG. 12. Photon loop diagrams that contribute to the $\tau^- \rightarrow (P_1 P_2)^- \nu_\tau$ decays.

where

$$\begin{aligned} \delta f_+(u) = & \frac{\alpha}{4\pi} \left[2 + \frac{1}{\varepsilon} - \gamma_E + \log 4\pi - \log \frac{m_\tau^2}{\mu^2} + (u - m_-^2) \mathcal{A}(u) + (u - m_-^2 - m_\tau^2) \mathcal{B}(u) \right. \\ & \left. + 2(m_-^2 + m_\tau^2 - u) \mathcal{C}(u, M_\gamma) + 2 \log \left(\frac{m_- m_\tau}{M_\gamma^2} \right) \right], \end{aligned} \quad (\text{B2})$$

$$\begin{aligned} \delta f_-(u) = & \frac{\alpha}{4\pi} \left[-5 - 3 \left(\frac{1}{\varepsilon} - \gamma_E + \log 4\pi \right) + \log \frac{m_-^2}{\mu^2} + 2 \log \frac{m_\tau^2}{\mu^2} + (3u + m_-^2 - 2m_\tau^2) \mathcal{A}(u) \right. \\ & \left. + (u + m_-^2 - m_\tau^2) \mathcal{B}(u) \right], \end{aligned} \quad (\text{B3})$$

with

$$\mathcal{A}(u) = \frac{1}{u} \left(-\frac{1}{2} \log r_\tau + \frac{2-y}{\sqrt{r_\tau}} \frac{x}{1-x^2} \log x \right), \quad (\text{B4})$$

$$\mathcal{B}(u) = \frac{1}{u} \left(\frac{1}{2} \log r_\tau + \frac{2r_\tau - y}{\sqrt{r_\tau}} \frac{x}{1-x^2} \log x \right), \quad (\text{B5})$$

$$\begin{aligned} \mathcal{C}(u, M_\gamma) = & \frac{1}{m_\tau m_-} \frac{x}{1-x^2} \left[-\frac{1}{2} \log^2 x + 2 \log x \log(1-x^2) - \frac{\pi^2}{6} + \frac{1}{8} \log^2 r_\tau \right. \\ & \left. + \text{Li}_2(x^2) + \text{Li}_2 \left(1 - \frac{x}{\sqrt{r_\tau}} \right) + \text{Li}_2(1 - x\sqrt{r_\tau}) - \log x \log \left(\frac{M_\gamma^2}{m_\tau m_-} \right) \right], \end{aligned} \quad (\text{B6})$$

and $C_V^{\pi\pi, KK, K^- \pi^0, K^0 \pi^-} = (\sqrt{2}, -1, \frac{1}{\sqrt{2}}, -1)$. Here, $\mathcal{A}(u)$, $\mathcal{B}(u)$ and $\mathcal{C}(u, M_\gamma)$ are written in terms of the variables

$$r_\tau = \frac{m_\tau^2}{m_-^2}, \quad y = 1 + r_\tau - \frac{u}{m_-^2}, \quad x = \frac{1}{2\sqrt{r_\tau}} \left(y - \sqrt{y^2 - 4r_\tau} \right), \quad (\text{B7})$$

and the dilogarithm

$$\text{Li}_2(x) = - \int_0^1 \frac{dt}{t} \log(1-xt). \quad (\text{B8})$$

The radiative corrections to these decays induce a dependence in the u variable. From a comparison with the results in Ref. [11], we get the following relation

$$\begin{aligned}\delta\bar{f}_+(u) &= \frac{\alpha}{4\pi} \frac{1}{f_+(0)} [\Gamma_1(u, m_\tau^2, m_-^2) + \Gamma_2(u, m_\tau^2, m_-^2)] + \dots \\ &= \frac{\alpha}{4\pi} \frac{1}{f_+(0)} [(u - m_-^2)\mathcal{A}(u) + (u - m_-^2 - m_\tau^2)\mathcal{B}(u)] + \dots,\end{aligned}\quad (\text{B9})$$

and

$$\begin{aligned}\delta\bar{f}_-(u) &= \frac{\alpha}{4\pi} \frac{1}{f_+(0)} [\Gamma_1(u, m_\tau^2, m_-^2) - \Gamma_2(u, m_\tau^2, m_-^2)] + \dots \\ &= \frac{\alpha}{4\pi} \frac{1}{f_+(0)} [(3u + m_-^2 - 2m_\tau^2)\mathcal{A}(u) + (u + m_-^2 - m_\tau^2)\mathcal{B}(u)] + \dots.\end{aligned}\quad (\text{B10})$$

Appendix C: $\tau^- \rightarrow (P_1 P_2)^- \nu_\tau$ decays

After the inclusion of the virtual-photon radiative corrections to the form factor in Sect. B, the amplitude for the $\tau^-(P) \rightarrow P_1^-(p_-) P_2^0(p_0) \nu_\tau(q')$ decays is given by

$$\mathcal{M}_0 = \frac{G_F V_{uD} \sqrt{S_{\text{EW}}}}{\sqrt{2}} H_V(p_-, p_0) \bar{u}(q') \gamma^\nu (1 - \gamma^5) u(P). \quad (\text{C1})$$

Thus, the spin-averaged squared amplitude follows

$$\begin{aligned}|\overline{\mathcal{M}_0}|^2 &= 2G_F^2 |V_{uD}|^2 S_{\text{EW}} \left\{ C_S^2 |F_0(t, u)|^2 D_0^{P^- P^0}(t, u) + C_S C_V \text{Re}[F_+(t, u) F_0^*(t, u)] D_{+0}^{P^- P^0}(t, u) \right. \\ &\quad \left. + C_V^2 |F_+(t, u)|^2 D_+^{P^- P^0}(t, u) \right\},\end{aligned}\quad (\text{C2})$$

where we have defined $F_{+/0}(t, u)$ in Eq. (32), and the expressions for $D_0^{P^- P^0}(t, u)$, $D_{+0}^{P^- P^0}(t, u)$ and $D_+^{P^- P^0}(t, u)$ are given in Eqs. (9)–(11).

The differential decay width in the tau rest frame is

$$\frac{d^2\Gamma}{dt du} = \frac{1}{32(2\pi)^3 m_\tau^3} |\overline{\mathcal{M}_0}|^2, \quad (\text{C3})$$

where $t = (p_- + p_0)^2$ is the invariant mass and $u = (P - p_-)^2 = (p_0 + k + q')^2$. The physical region is limited by $(m_- + m_0)^2 \leq t \leq m_\tau^2$ and $u^-(t) \leq u \leq u^+(t)$, with

$$u^\pm(t) = \frac{1}{2t} \left[2t(m_\tau^2 + m_0^2 - t) - (m_\tau^2 - t)(t + m_-^2 - m_0^2) \pm (m_\tau^2 - t) \sqrt{\lambda(t, m_-^2, m_0^2)} \right], \quad (\text{C4})$$

and $\lambda(x, y, z) = x^2 + y^2 + z^2 - 2xy - 2xz - 2yz$.

The invariant mass distribution is obtained integrating upon the u variable

$$\begin{aligned} \frac{d\Gamma}{dt} = & \frac{G_F^2 S_{EW} |V_{uD}|^2 m_\tau^3}{384\pi^3 t} \left\{ \frac{1}{2t^2} \left(1 - \frac{t}{m_\tau^2}\right)^2 \lambda^{1/2}(t, m_-^2, m_0^2) \right. \\ & \times \left[C_V^2 |F_+(t)|^2 \left(1 + \frac{2t}{m_\tau^2}\right) \lambda(t, m_-^2, m_0^2) \left(1 + \tilde{\delta}_+(t)\right) + 3C_S^2 \Delta_{-0}^2 |F_0(t)|^2 \left(1 + \tilde{\delta}_0(t)\right) \right] \\ & \left. + C_S C_V \frac{4}{\sqrt{t}} \tilde{\delta}_{+0}(t) \right\}, \end{aligned} \quad (\text{C5})$$

where

$$\tilde{\delta}_0(t) = \frac{\int_{u^-(t)}^{u^+(t)} D_0^{P^- P^0}(t, u) 2\text{Re} [F_0(t) \delta F_0^*(t, u)] du}{\int_{u^-(t)}^{u^+(t)} D_0^{P^- P^0}(t, u) |F_0(t)|^2 du}, \quad (\text{C6a})$$

$$\tilde{\delta}_+(t) = \frac{\int_{u^-(t)}^{u^+(t)} D_+^{P^- P^0}(t, u) 2\text{Re} [F_+(t) \delta F_+^*(u)] du}{\int_{u^-(t)}^{u^+(t)} D_+^{P^- P^0}(t, u) |F_+(t)|^2 du}, \quad (\text{C6b})$$

$$\tilde{\delta}_{+0}(t) = \frac{3t\sqrt{t}}{4m_\tau^6} \int_{u^-(t)}^{u^+(t)} D_{+0}^{P^- P^0}(t, u) (\text{Re} [F_+(t) \delta F_0^*(t, u)] + \text{Re} [F_0(t) \delta F_+^*(u)]) du. \quad (\text{C6c})$$

Appendix D: Kinematics

As in Refs. [11, 51, 53, 109], after an integration over $\mathcal{D}_{\text{IV/III}}$ and \mathcal{D}_{III} , the functions in Eqs. (14) are given by (we note that K_{11} is numerically negligible)

$$J_{11}(t, u) = \log \left(\frac{2x_+(t, u) \bar{Y}}{M_\gamma} \right) \frac{1}{\bar{\beta}} \log \left(\frac{1 + \bar{\beta}}{1 - \bar{\beta}} \right) \quad (\text{D1a})$$

$$+ \frac{1}{\bar{\beta}} [\text{Li}_2(1/Y_2) - \text{Li}_2(Y_1) + \log^2(-1/Y_2)/4 - \log^2(-1/Y_1)/4], \quad (\text{D1b})$$

$$J_{20}(t, u) = \log \left(\frac{M_\gamma(m_\tau^2 - t)}{m_\tau x_+(t, u)} \right), \quad (\text{D1c})$$

$$J_{02}(t, u) = \log \left(\frac{M_\gamma(m_\tau^2 + m_0^2 - t - u)}{m_- x_+(t, u)} \right), \quad (\text{D1d})$$

$$K_{20}(t, u) = K_{02}(t, u) = \log \left(\frac{x_-(t, u)}{x_+(t, u)} \right), \quad (\text{D1e})$$

where

$$\begin{aligned} x_\pm(t, u) = & \frac{-m_-^4 + (m_0^2 - t)(m_\tau^2 - u) + m_-^2(m_\tau^2 + m_0^2 + t + u)}{2m_-^2} \\ & \pm \frac{\lambda^{1/2}(u, m_\tau^2, m_-^2) \lambda^{1/2}(t, m_-^2, m_0^2)}{2m_-^2}. \end{aligned} \quad (\text{D2})$$

These expressions are written in terms of

$$Y_{1,2} = \frac{1 - 2\bar{\alpha} \pm \sqrt{(1 - 2\bar{\alpha})^2 - (1 - \bar{\beta}^2)}}{1 + \bar{\beta}}, \quad (\text{D3})$$

with

$$\begin{aligned} \bar{\alpha} &= \frac{(m_\tau^2 - t)(m_\tau^2 + m_0^2 - t - u)}{(m_-^2 + m_\tau^2 - u)} \cdot \frac{\lambda(u, m_-^2, m_\tau^2)}{2\bar{\delta}}, \\ \bar{\beta} &= -\frac{\sqrt{\lambda(u, m_-^2, m_\tau^2)}}{m_-^2 + m_\tau^2 - u}, \\ \bar{\gamma} &= \frac{\sqrt{\lambda(u, m_-^2, m_\tau^2)}}{2\sqrt{\bar{\delta}}}, \\ \bar{\delta} &= -m_0^4 m_\tau^2 + m_-^2 (m_\tau^2 - t)(m_0^2 - u) - tu(-m_\tau^2 + t + u) \\ &\quad + m_0^2(-m_\tau^4 + tu + m_\tau^2 t + m_\tau^2 u). \end{aligned}$$

-
- [1] Michel Davier, Andreas Hocker, and Zhiqing Zhang. The Physics of Hadronic Tau Decays. *Rev. Mod. Phys.*, 78:1043–1109, 2006.
 - [2] Antonio Pich. Precision Tau Physics. *Prog. Part. Nucl. Phys.*, 75:41–85, 2014.
 - [3] Y. Aoki et al. FLAG Review 2021. *Eur. Phys. J. C*, 82(10):869, 2022.
 - [4] A. Pich and J. Portoles. The Vector form-factor of the pion from unitarity and analyticity: A Model independent approach. *Phys. Rev. D*, 63:093005, 2001.
 - [5] D. Gómez Dumm and P. Roig. Dispersive representation of the pion vector form factor in $\tau \rightarrow \pi\pi\nu_\tau$ decays. *Eur. Phys. J. C*, 73(8):2528, 2013.
 - [6] Sergi González-Solís and Pablo Roig. A dispersive analysis of the pion vector form factor and $\tau^- \rightarrow K^- K_S \nu_\tau$ decay. *Eur. Phys. J. C*, 79(5):436, 2019.
 - [7] Matthias Jamin, Jose Antonio Oller, and Antonio Pich. Strangeness changing scalar form-factors. *Nucl. Phys. B*, 622:279–308, 2002.
 - [8] B. Moussallam. Analyticity constraints on the strangeness changing vector current and applications to $\tau \rightarrow K\pi\nu_\tau$, $\tau \rightarrow K\pi\pi\nu_\tau$. *Eur. Phys. J. C*, 53:401–412, 2008.
 - [9] Diogo R. Boito, Rafel Escribano, and Matthias Jamin. $K\pi$ vector form-factor, dispersive constraints and $\tau \rightarrow \nu_\tau K\pi$ decays. *Eur. Phys. J. C*, 59:821–829, 2009.

- [10] D. R. Boito, R. Escribano, and M. Jamin. $K\pi$ vector form factor constrained by $\tau \rightarrow K\pi\nu_\tau$ and K_{l3} decays. *JHEP*, 09:031, 2010.
- [11] Mario Antonelli, Vincenzo Cirigliano, Alberto Lusiani, and Emilie Passemar. Predicting the τ strange branching ratios and implications for V_{us} . *JHEP*, 10:070, 2013.
- [12] V. Bernard. First determination of $f_+(0)|V_{us}|$ from a combined analysis of $\tau \rightarrow K\pi\nu_\tau$ decay and πK scattering with constraints from K_{l3} decays. *JHEP*, 06:082, 2014.
- [13] R. Escribano, S. Gonzalez-Solis, and P. Roig. $\tau^- \rightarrow K^- \eta^{(\prime)} \nu_\tau$ decays in Chiral Perturbation Theory with Resonances. *JHEP*, 10:039, 2013.
- [14] R. Escribano, S. González-Solís, M. Jamin, and P. Roig. Combined analysis of the decays $\tau^- \rightarrow K_S \pi^- \nu_\tau$ and $\tau^- \rightarrow K^- \eta \nu_\tau$. *JHEP*, 09:042, 2014.
- [15] S. Descotes-Genon and B. Moussallam. Analyticity of $\eta\pi$ isospin-violating form factors and the $\tau \rightarrow \eta\pi\nu$ second-class decay. *Eur. Phys. J. C*, 74:2946, 2014.
- [16] Rafel Escribano, Sergi Gonzalez-Solis, and Pablo Roig. Predictions on the second-class current decays $\tau^- \rightarrow \pi^- \eta^{(\prime)} \nu_\tau$. *Phys. Rev. D*, 94(3):034008, 2016.
- [17] G. Abbiendi et al. A Study of one prong tau decays with a charged kaon. *Eur. Phys. J. C*, 19:653–665, 2001.
- [18] S. Schael et al. Branching ratios and spectral functions of tau decays: Final ALEPH measurements and physics implications. *Phys. Rept.*, 421:191–284, 2005.
- [19] Bernard Aubert et al. Measurements of Charged Current Lepton Universality and $|V_{us}|$ using Tau Lepton Decays to $e^- \bar{\nu}_e \nu_\tau$, $\mu^- \bar{\nu}_\mu \nu_\tau$, $\pi^- \nu_\tau$, and $K^- \nu_\tau$. *Phys. Rev. Lett.*, 105:051602, 2010.
- [20] K. Ackerstaff et al. Measurement of the strong coupling constant α_s and the vector and axial vector spectral functions in hadronic tau decays. *Eur. Phys. J. C*, 7:571–593, 1999.
- [21] S. Anderson et al. Hadronic structure in the decay $\tau^- \rightarrow \pi^- \pi^0 \nu_\tau$. *Phys. Rev. D*, 61:112002, 2000.
- [22] M. Fujikawa et al. High-Statistics Study of the $\tau^- \rightarrow \pi^- \pi^0 \nu_\tau$ Decay. *Phys. Rev. D*, 78:072006, 2008.
- [23] J. P. Lees et al. Measurement of the spectral function for the $\tau^- \rightarrow K^- K_S \nu_\tau$ decay. *Phys. Rev. D*, 98(3):032010, 2018.
- [24] Y. Jin et al. Observation of $\tau^- \rightarrow \pi^- \nu_\tau e^+ e^-$ and search for $\tau^- \rightarrow \pi^- \nu_\tau \mu^+ \mu^-$. *Phys. Rev. D*, 100(7):071101, 2019.
- [25] D. Gomez Dumm, A. Pich, and J. Portoles. $\tau \rightarrow \pi\pi\pi\nu_\tau$ decays in the resonance effective theory. *Phys. Rev. D*, 69:073002, 2004.

- [26] D. Gomez Dumm, P. Roig, A. Pich, and J. Portoles. $\tau \rightarrow \pi\pi\pi\nu_\tau$ decays and the $a(1)(1260)$ off-shell width revisited. *Phys. Lett. B*, 685:158–164, 2010.
- [27] D. Gomez Dumm, P. Roig, A. Pich, and J. Portoles. Hadron structure in $\tau \rightarrow KK\pi\nu_\tau$ decays. *Phys. Rev. D*, 81:034031, 2010.
- [28] Daniel Gomez Dumm and Pablo Roig. Resonance Chiral Lagrangian analysis of $\tau^- \rightarrow \eta^{(\prime)}\pi^-\pi^0\nu_\tau$ decays. *Phys. Rev. D*, 86:076009, 2012.
- [29] O. Shekhovtsova, T. Przedzinski, P. Roig, and Z. Was. Resonance chiral Lagrangian currents and τ decay Monte Carlo. *Phys. Rev. D*, 86:113008, 2012.
- [30] I. M. Nugent, T. Przedzinski, P. Roig, O. Shekhovtsova, and Z. Was. Resonance chiral Lagrangian currents and experimental data for $\tau^- \rightarrow \pi^-\pi^-\pi^+\nu_\tau$. *Phys. Rev. D*, 88:093012, 2013.
- [31] Juan Jose Sanz-Cillero and Olga Shekhovtsova. Refining the scalar and tensor contributions in $\tau \rightarrow \pi\pi\pi\nu_\tau$ decays. *JHEP*, 12:080, 2017.
- [32] M. Mikhasenko, A. Pilloni, M. Albaladejo, C. Fernández-Ramírez, A. Jackura, V. Mathieu, J. Nys, A. Rodas, B. Ketzer, and A. P. Szczepaniak. Pole position of the $a_1(1260)$ from τ -decay. *Phys. Rev. D*, 98(9):096021, 2018.
- [33] Saray Arteaga, Ling-Yun Dai, Adolfo Guevara, and Pablo Roig. Tension between $e^+e^- \rightarrow \eta\pi^-\pi^+$ and $\tau^- \rightarrow \eta\pi^-\pi^0\nu_\tau$ data and nonstandard interactions. *Phys. Rev. D*, 106(9):096016, 2022.
- [34] E. A. Garcés, M. Hernández Villanueva, G. López Castro, and P. Roig. Effective-field theory analysis of the $\tau^- \rightarrow \eta^{(\prime)}\pi^-\nu_\tau$ decays. *JHEP*, 12:027, 2017.
- [35] Vincenzo Cirigliano, Andreas Crivellin, and Martin Hoferichter. No-go theorem for nonstandard explanations of the $\tau \rightarrow K_S\pi\nu_\tau$ CP asymmetry. *Phys. Rev. Lett.*, 120(14):141803, 2018.
- [36] J. A. Miranda and P. Roig. Effective-field theory analysis of the $\tau^- \rightarrow \pi^-\pi^0\nu_\tau$ decays. *JHEP*, 11:038, 2018.
- [37] Vincenzo Cirigliano, Adam Falkowski, Martín González-Alonso, and Antonio Rodríguez-Sánchez. Hadronic τ Decays as New Physics Probes in the LHC Era. *Phys. Rev. Lett.*, 122(22):221801, 2019.
- [38] Javier Rendón, Pablo Roig, and Genaro Toledo Sánchez. Effective-field theory analysis of the $\tau^- \rightarrow (K\pi)^-\nu_\tau$ decays. *Phys. Rev. D*, 99(9):093005, 2019.
- [39] Feng-Zhi Chen, Xin-Qiang Li, Ya-Dong Yang, and Xin Zhang. CP asymmetry in $\tau \rightarrow K_S\pi\nu_\tau$ decays within the Standard Model and beyond. *Phys. Rev. D*, 100(11):113006, 2019.
- [40] Sergi González-Solís, Alejandro Miranda, Javier Rendón, and Pablo Roig. Effective-field theory analysis of the $\tau^- \rightarrow K^-(\eta^{(\prime)}, K^0)\nu_\tau$ decays. *Phys. Rev. D*, 101(3):034010, 2020.

- [41] Sergi González-Solís, Alejandro Miranda, Javier Rendón, and Pablo Roig. Exclusive hadronic tau decays as probes of non-SM interactions. *Phys. Lett. B*, 804:135371, 2020.
- [42] Feng-Zhi Chen, Xin-Qiang Li, and Ya-Dong Yang. CP asymmetry in the angular distribution of $\tau \rightarrow K_S \pi \nu_\tau$ decays. *JHEP*, 05:151, 2020.
- [43] M. A. Arroyo-Ureña, G. Hernández-Tomé, G. López-Castro, P. Roig, and I. Rosell. One-loop determination of $\tau \rightarrow \pi(K) \nu_\tau[\gamma]$ branching ratios and new physics tests. *JHEP*, 02:173, 2022.
- [44] M. A. Arroyo-Ureña, G. Hernández-Tomé, G. López-Castro, P. Roig, and I. Rosell. Radiative corrections to $\tau \rightarrow \pi(K) \nu_\tau[\gamma]$: A reliable new physics test. *Phys. Rev. D*, 104(9):L091502, 2021.
- [45] Feng-Zhi Chen, Xin-Qiang Li, Shi-Can Peng, Ya-Dong Yang, and Hong-Hao Zhang. CP asymmetry in the angular distributions of $\tau \rightarrow K_S \pi \nu_\tau$ decays. Part II. General effective field theory analysis. *JHEP*, 01:108, 2022.
- [46] Vincenzo Cirigliano, David Díaz-Calderón, Adam Falkowski, Martín González-Alonso, and Antonio Rodríguez-Sánchez. Semileptonic tau decays beyond the Standard Model. *JHEP*, 04:152, 2022.
- [47] Zhi-Hui Guo and Pablo Roig. One meson radiative tau decays. *Phys. Rev. D*, 82:113016, 2010.
- [48] A. Guevara, G. López Castro, and P. Roig. Weak radiative pion vertex in $\tau^- \rightarrow \pi^- \nu_\tau \ell^+ \ell^-$ decays. *Phys. Rev. D*, 88(3):033007, 2013.
- [49] Adolfo Guevara, Gabriel López Castro, and Pablo Roig. Improved description of dilepton production in $\tau^- \rightarrow \nu_\tau P^-$ decays. *Phys. Rev. D*, 105(7):076007, 2022.
- [50] V. Cirigliano, G. Ecker, and H. Neufeld. Isospin violation and the magnetic moment of the muon. *Phys. Lett.*, B513:361–370, 2001.
- [51] V. Cirigliano, G. Ecker, and H. Neufeld. Radiative tau decay and the magnetic moment of the muon. *JHEP*, 08:002, 2002.
- [52] F. Flores-Baez, A. Flores-Tlalpa, G. Lopez Castro, and G. Toledo Sanchez. Long-distance radiative corrections to the di-pion tau lepton decay. *Phys. Rev. D*, 74:071301, 2006.
- [53] J. A. Miranda and P. Roig. New τ -based evaluation of the hadronic contribution to the vacuum polarization piece of the muon anomalous magnetic moment. *Phys. Rev. D*, 102:114017, 2020.
- [54] J. L. Gutiérrez Santiago, G. López Castro, and P. Roig. Lepton-pair production in dipion τ lepton decays. *Phys. Rev. D*, 103(1):014027, 2021.
- [55] Cheng Chen, Chun-Gui Duan, and Zhi-Hui Guo. Triple-product asymmetry in the radiative two-pion tau decay. *JHEP*, 08:144, 2022.

- [56] Pere Masjuan, Alejandro Miranda, and Pablo Roig. τ data-driven evaluation of Euclidean windows for the hadronic vacuum polarization. 5 2023.
- [57] F. V. Flores-Baéz and J. R. Morones-Ibarra. Model Independent Electromagnetic corrections in hadronic τ decays. *Phys. Rev. D*, 88(7):073009, 2013.
- [58] A. Guevara, G. López-Castro, and P. Roig. $\tau^- \rightarrow \eta^{(\prime)} \pi^- \nu_\tau \gamma$ decays as backgrounds in the search for second class currents. *Phys. Rev.*, D95(5):054015, 2017.
- [59] F. E. Low. Bremsstrahlung of very low-energy quanta in elementary particle collisions. *Phys. Rev.*, 110:974–977, 1958.
- [60] A. Sirlin. Radiative corrections to G_V/G_μ in simple extensions of the $SU(2) \times U(1)$ gauge model. *Nucl. Phys. B*, 71:29–51, 1974.
- [61] A. Sirlin. Current Algebra Formulation of Radiative Corrections in Gauge Theories and the Universality of the Weak Interactions. *Rev. Mod. Phys.*, 50:573, 1978. [Erratum: *Rev. Mod. Phys.* 50, 905 (1978)].
- [62] A. Sirlin. Large m_W, m_Z Behavior of the $O(\alpha)$ Corrections to Semileptonic Processes Mediated by W . *Nucl. Phys. B*, 196:83–92, 1982.
- [63] W. J. Marciano and A. Sirlin. Radiative Corrections to beta Decay and the Possibility of a Fourth Generation. *Phys. Rev. Lett.*, 56:22, 1986.
- [64] W. J. Marciano and A. Sirlin. Electroweak Radiative Corrections to tau Decay. *Phys. Rev. Lett.*, 61:1815–1818, 1988.
- [65] William J. Marciano and A. Sirlin. Radiative corrections to $\pi_{\ell 2}$ decays. *Phys. Rev. Lett.*, 71:3629–3632, 1993.
- [66] Eric Braaten and Chong-Sheng Li. Electroweak radiative corrections to the semihadronic decay rate of the tau lepton. *Phys. Rev. D*, 42:3888–3891, 1990.
- [67] Jens Erler. Electroweak radiative corrections to semileptonic tau decays. *Rev. Mex. Fis.*, 50:200–202, 2004.
- [68] T. H. Burnett and Norman M. Kroll. Extension of the low soft photon theorem. *Phys. Rev. Lett.*, 20:86, 1968.
- [69] Vincenzo Cirigliano, Maurizio Giannotti, and Helmut Neufeld. Electromagnetic effects in $K_{\ell 3}$ decays. *JHEP*, 11:006, 2008.
- [70] Mattia Bruno, Taku Izubuchi, Christoph Lehner, and Aaron Meyer. On isospin breaking in τ decays for $(g-2)_\mu$ from Lattice QCD. *PoS, LATTICE2018*:135, 2018.

- [71] Steven Weinberg. Phenomenological Lagrangians. *Physica A*, 96(1-2):327–340, 1979.
- [72] J. Gasser and H. Leutwyler. Chiral Perturbation Theory to One Loop. *Annals Phys.*, 158:142, 1984.
- [73] J. Gasser and H. Leutwyler. Chiral Perturbation Theory: Expansions in the Mass of the Strange Quark. *Nucl. Phys. B*, 250:465–516, 1985.
- [74] Johan Bijnens, Gilberto Colangelo, and Gerhard Ecker. The Mesonic chiral Lagrangian of order p^6 . *JHEP*, 02:020, 1999.
- [75] J. Bijnens, L. Girlanda, and P. Talavera. The Anomalous chiral Lagrangian of order p^6 . *Eur. Phys. J. C*, 23:539–544, 2002.
- [76] G. Ecker, J. Gasser, A. Pich, and E. de Rafael. The Role of Resonances in Chiral Perturbation Theory. *Nucl. Phys.*, B321:311–342, 1989.
- [77] G. Ecker, J. Gasser, H. Leutwyler, A. Pich, and E. de Rafael. Chiral Lagrangians for Massive Spin 1 Fields. *Phys. Lett.*, B223:425–432, 1989.
- [78] J. Portoles. Basics of Resonance Chiral Theory. *AIP Conf. Proc.*, 1322(1):178–187, 2010.
- [79] J. Wess and B. Zumino. Consequences of anomalous Ward identities. *Phys. Lett.*, 37B:95–97, 1971.
- [80] Edward Witten. Global Aspects of Current Algebra. *Nucl. Phys.*, B223:422–432, 1983.
- [81] V. Cirigliano, G. Ecker, M. Eidemuller, Roland Kaiser, A. Pich, and J. Portoles. Towards a consistent estimate of the chiral low-energy constants. *Nucl. Phys.*, B753:139–177, 2006.
- [82] Karol Kampf and Jiri Novotny. Resonance saturation in the odd-intrinsic parity sector of low-energy QCD. *Phys. Rev.*, D84:014036, 2011.
- [83] A. Pich. Colorless mesons in a polychromatic world. In *The Phenomenology of Large $N(c)$ QCD*, pages 239–258, 5 2002.
- [84] Gerard 't Hooft. A Planar Diagram Theory for Strong Interactions. *Nucl. Phys. B*, 72:461, 1974.
- [85] Gerard 't Hooft. A Two-Dimensional Model for Mesons. *Nucl. Phys. B*, 75:461–470, 1974.
- [86] J. J. Sakurai. Theory of strong interactions. *Annals Phys.*, 11:1–48, 1960.
- [87] Masako Bando, Taichiro Kugo, and Koichi Yamawaki. Nonlinear Realization and Hidden Local Symmetries. *Phys. Rept.*, 164:217–314, 1988.
- [88] P. Roig, A. Guevara, and G. López Castro. $VV'P$ form factors in resonance chiral theory and the $\pi - \eta - \eta'$ light-by-light contribution to the muon $g - 2$. *Phys. Rev. D*, 89(7):073016, 2014.
- [89] V. Cirigliano, G. Ecker, H. Neufeld, and A. Pich. Meson resonances, large $N(c)$ and chiral symmetry. *JHEP*, 06:012, 2003.

- [90] Zhi-Hui Guo and Juan Jose Sanz-Cillero. $\pi\pi$ -scattering lengths at $O(p^{**6})$ revisited. *Phys. Rev. D*, 79:096006, 2009.
- [91] Pablo Roig and Pablo Sanchez-Puertas. Axial-vector exchange contribution to the hadronic light-by-light piece of the muon anomalous magnetic moment. *Phys. Rev. D*, 101(7):074019, 2020.
- [92] R. L. Workman et al. Review of Particle Physics. *PTEP*, 2022:083C01, 2022.
- [93] A. Guevara, P. Roig, and J. J. Sanz-Cillero. Pseudoscalar pole light-by-light contributions to the muon $(g-2)$ in Resonance Chiral Theory. *JHEP*, 06:160, 2018.
- [94] D. Gomez Dumm, A. Pich, and J. Portoles. The Hadronic off-shell width of meson resonances. *Phys. Rev. D*, 62:054014, 2000.
- [95] J. Bijnens, G. Ecker, and J. Gasser. Radiative semileptonic kaon decays. *Nucl. Phys.*, B396:81–118, 1993.
- [96] V. Cirigliano, G. Ecker, M. Eidemuller, A. Pich, and J. Portoles. The $\langle VAP \rangle$ Green function in the resonance region. *Phys. Lett. B*, 596:96–106, 2004.
- [97] Pablo Roig and Juan José Sanz Cillero. Consistent high-energy constraints in the anomalous QCD sector. *Phys. Lett. B*, 733:158–163, 2014.
- [98] Zhi-Hui Guo and J. A. Oller. Resonances from meson-meson scattering in $U(3)$ CHPT. *Phys. Rev. D*, 84:034005, 2011.
- [99] Zhi-Hui Guo, J. A. Oller, and J. Ruiz de Elvira. Chiral dynamics in form factors, spectral-function sum rules, meson-meson scattering and semi-local duality. *Phys. Rev. D*, 86:054006, 2012.
- [100] Zhi-Hui Guo, Liuming Liu, Ulf-G. Meißner, J. A. Oller, and A. Rusetsky. Chiral study of the $a_0(980)$ resonance and $\pi\eta$ scattering phase shifts in light of a recent lattice simulation. *Phys. Rev. D*, 95(5):054004, 2017.
- [101] Leonardo Esparza-Arellano, Antonio Rojas, and Genaro Toledo. Sizing the double pole resonant enhancement in $e^+e^- \rightarrow \pi^0\pi^0\gamma$ cross section and $\tau^- \rightarrow \pi^-\pi^0\nu_\tau\gamma$ decay. 8 2023.
- [102] V. Cirigliano, M. Knecht, H. Neufeld, H. Rupertsberger, and P. Talavera. Radiative corrections to $K_{\ell 3}$ decays. *Eur. Phys. J. C*, 23:121–133, 2002.
- [103] Yasmine Sara Amhis et al. Averages of b-hadron, c-hadron, and τ -lepton properties as of 2021. *Phys. Rev. D*, 107(5):052008, 2023.
- [104] Vincenzo Cirigliano, James Jenkins, and Martin Gonzalez-Alonso. Semileptonic decays of light quarks beyond the Standard Model. *Nucl. Phys. B*, 830:95–115, 2010.

- [105] Tanmoy Bhattacharya, Vincenzo Cirigliano, Saul D. Cohen, Alberto Filipuzzi, Martin Gonzalez-Alonso, Michael L. Graesser, Rajan Gupta, and Huey-Wen Lin. Probing Novel Scalar and Tensor Interactions from (Ultra)Cold Neutrons to the LHC. *Phys. Rev. D*, 85:054512, 2012.
- [106] G. D’Ambrosio, G. F. Giudice, G. Isidori, and A. Strumia. Minimal flavor violation: An Effective field theory approach. *Nucl. Phys. B*, 645:155–187, 2002.
- [107] Yasmine Sara Amhis et al. Averages of b-hadron, c-hadron, and τ -lepton properties as of 2021. *Phys. Rev. D*, 107(5):052008, 2023.
- [108] V. Cirigliano, H. Neufeld, and H. Pichl. K_{e3} decays and CKM unitarity. *Eur. Phys. J. C*, 35:53–65, 2004.
- [109] Alain Flores-Tlalpa. *Modelo de dominancia de mesones para decaimientos semileptónicos de sabores pesados*. PhD thesis, CINVESTAV, IPN, 2008.